Journal of Mineralogical and Petrological Sciences, Volume 116, page 26–44, 2021

Ore and skarn mineralogy of the Eboshi deposit of the Naganobori copper mine, Yamaguchi, Japan

Mariko NAGASHIMA[*], Yukina MORISHITA[**,***], Yuji IMOTO[**,†] and Teruyoshi IMAOKA[*]

[*]*Division of Earth Science, Graduate School of Science and Technology for Innovation, Yamaguchi University, Yamaguchi 753–8512, Japan*
[**]*Department of Geosphere Science, Faculty of Science, Yamaguchi University, Yamaguchi 753–8512, Japan*
[***]*Fujiyama Ltd., Motoshiro–cho 216–19, Naka–ku, Hamamatsu, Shizuoka 430–0946, Japan*
[†]*TOKOGEOTECH CORPORATION, 9–10–1 Iida Hachihonmatsu, Higashihiroshima, Hiroshima 739–0146, Japan*

Mineral assemblages and chemical compositions of ore minerals from the Eboshi deposit, the historical Naganobori copper mine, Yamaguchi Prefecture, Japan were investigated in order to clarify its characteristics as a skarn deposit. Some Bi–, Ag–, and Te–bearing minerals are newly identified, which contribute updating the mineralization sequence of this deposit. Samples collected from the mine dump are one massive magnetite ore, and copper ores associated with skarn gangue minerals. Skarns are categorized as clinopyroxene skarn, garnet skarn, and wollastonite skarn, and the clinopyroxene skarn is the most dominant. The major ore minerals are chalcopyrite, cobaltite, and early–stage pyrite (Py–I) and later stage pyrite (Py–II). Py–II is enriched in arsenic (~ 5.19 As wt%). The Bi–, Ag–, and Te–bearing minerals, such as native bismuth, bismuthinite, wittichenite, emplectite, tsumoite, kawazulite, hessite, and matildite are minor ore minerals. Based on the mineral assemblages and textures of the specimens examined, four ore mineralization stages were recognized; the ore mineralization stage I is characterized by the major ore minerals such as chalcopyrite, bornite, pyrrhotite, sphalerite, and Py–I. The stage II is defined by the mineralization of cobaltite, Py–II, and Bi(–Cu)–bearing sulfides such as native bismuth, bismuthinite, and wittichenite. The mineralization stage III is characterized by the Ag– and/or Te–bearing ore minerals such as matildite, kawazulite, tsumoite, and hessite. The stage IV is characterized by chalcopyrite veins cutting the main skarn masses and the host limestone. The mineralogical properties and mineralization process of the Eboshi deposit is similar to those of the skarn deposits in the Yamato mine and the Tsumo mine, and consistent with common skarn–type deposits associated with ilmenite–series granitoids in the San–yo Belt, which are characterized by the occurrence of minor Ag– and/or Te–bearing ore minerals.

Keywords: Naganobori, Eboshi, Yamaguchi, skarn, Cobalt, Ilmenite–series

INTRODUCTION

Most Japanese skarn deposits are genetically related to felsic magmatic activity of Cretaceous or Miocene age (Shimazaki, 1980). Skarn deposits of Cretaceous to Paleogene age associated with the Sanyo–Naegi granitic activity are distributed in the Sanyo–Naegi Belt within the Inner Zone in SW Japan (Shimazaki, 1968, 1980). Not a few skarn deposits occur in and around the Akiyoshi Plateau located in the central Yamaguchi Prefecture. These skarn deposits occur in Paleozoic accretionary complexes comprising the Akiyoshi Limestone Group and were generated by the intrusions of Cretaceous ilmenite–series granitic magma into the limestone (Kato, 1916; Ogura, 1921; Suzuki, 1932; Kato, 1937; Watanabe, 2009). Among them, the skarn deposits forming the Naganobori, Kitabira, Yamato, and Sanjo mines are main ones (Fig. 1a).

The Naganobori mine is one of the oldest copper mines in Japan and was operated from the eighth century to 1960 (e.g., Ueda, 2002). Kato (1916) reported that 1144 tons of copper was produced from the Umegakubo and Oda deposits of the Naganobori mine (Fig. 1b) in the period between 1908 and 1912. The Cu content in copper concentrates attains 7.1% (Ogura, 1921). The Naganobori skarn type copper deposits is related to granitic rocks known as the Hanano–yama granite porphyry (Figs. 1a and 1b). Intense hydrothermal activity in the Hanano–

doi:10.2465/jmps.200818
M. Nagashima, nagashim@yamaguchi–u.ac.jp Corresponding author

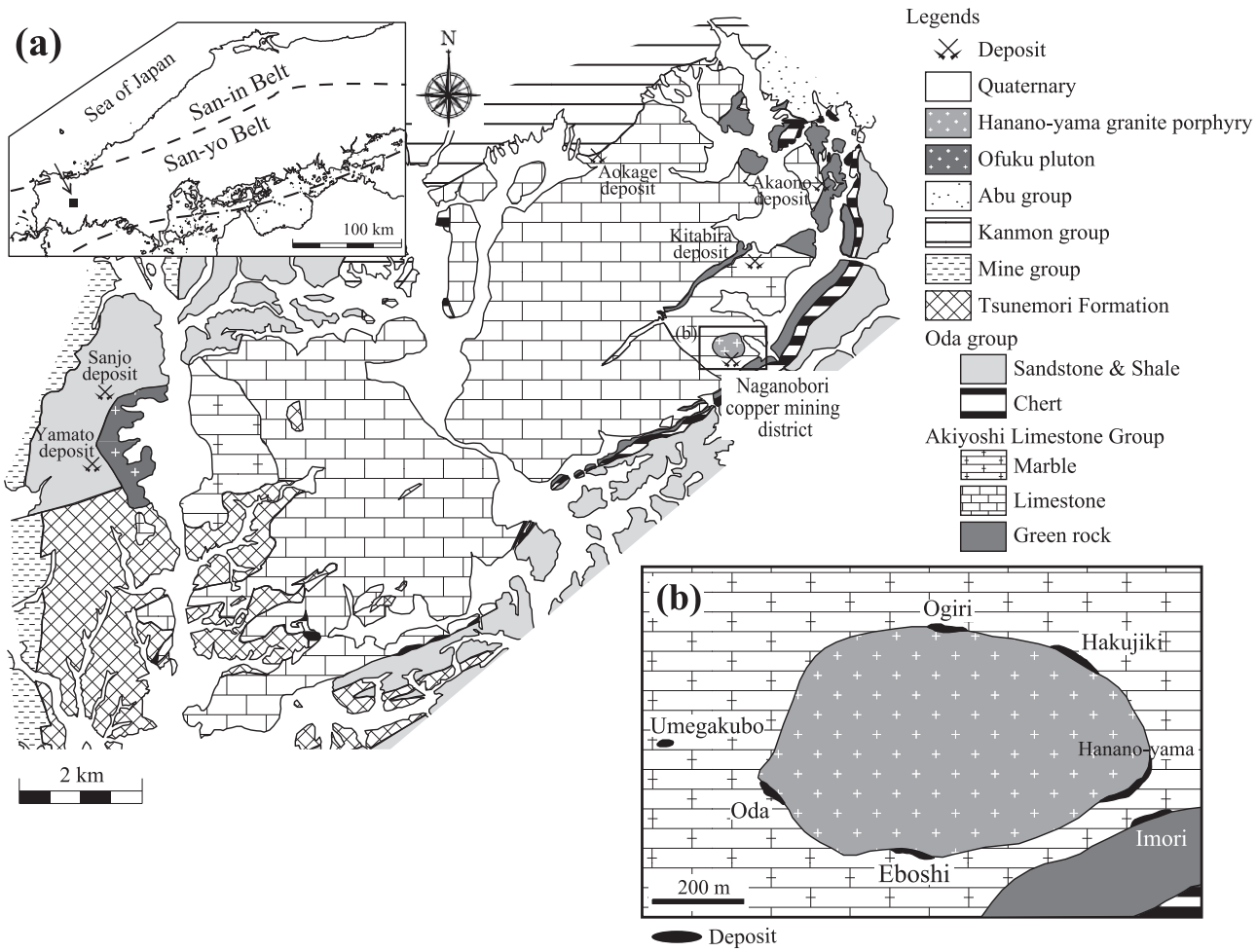

Figure 1. (a) Geological map of the Akiyoshi Plateau and surrounding area modified from Ota (1976). (b) The Naganobori mining district. Distribution of the Hanano-yama granite porphyry and representative deposits in (b) are after Kato (1916).

yama granite porphyry has been proved by abundant fluid inclusions with varying vapor/liquid ratios (Sasaki et al., 2014). Sasaki et al. (2014) reported the extremely high Cu contents (~ 484 ppm) of the Hanano-yama granite porphyry, which far exceed those of San-yo Belt ilmenite-series granitoids (average 5.5 ppm). According to Hirabayashi (1909), cobaltite concentration in the Eboshi deposit was found in 1908. Co-rich ores with more than 10 wt% Co were mined in the history (Nakamura, 1954). The geology and mineralization of the Naganobori skarn deposits were studied by Kato (1916) and Ogura (1921). Kato (1916) concluded that the major ore minerals in the Eboshi deposit, such as chalcopyrite, pyrrhotite, bornite, and scheelite, were formed at the early stage of the mineralization; cobaltite and native bismuth in the quartz veinlets were crystallized at the later stage, and chalcopyrite veins cutting the main skarn masses and the host limestone were formed at the latest stage. Ogura (1921) described ore minerals such as chalcopyrite, cobaltite, scheelite, magnetite, pyrrhotite, tetrahedrite, and gangue minerals of hedenbergite, garnet, quartz, and calcite. In addition to the studies cited above, Watanabe (2009) reported cobaltite, bismuthinite, native bismuth, electrum, stannoidite, mawsonite, wittichenite, pavonite, joséite, and scheelite from the Naganobori copper skarn deposits, accompanying major chalcopyrite and pyrrhotite, and minor bornite, sphalerite, galena, and magnetite. However, the occurrences of the Bi-, Ag-, and Co-minerals in the Naganobori copper skarn deposit have not been described in detail. Nagashima et al. (2016) studied ore and skarn mineralogy of the Yamato skarn deposit in Akiyoshi limestones across from the Naganobori copper skarn deposit (Fig. 1a). They clarified presence of Ag-, Bi-, Co-, and Ni-bearing ore minerals such as argentite, matildite, bismuthinite, stannite, stannoidite, violarite, cobaltite, gersdorffite, and native gold, in addition to the known main ore minerals (pyrite, chalcopyrite, pyrrhotite, arsenopyrite, galena, sphalerite, and native bismuth), and in-

dicated that the Bi-, Ag-, Co-, and Ni-mineralization occurred in the middle stage of mineralization characterized by major ore minerals. Such accessory ore minerals including Ag-, Bi-, Co-, and Ni-bearing minerals also occur in the skarn deposits forming the Tsumo mine, Shimane Prefecture (e.g., Sugaki et al., 1981), where Cu-Zn-W skarn deposit related to the magnetite-series Tsumo monzodiorite-granite porphyry complex, and Sn-W mineralization is supposed to be related to the ilmenite-series Maruyama granite porphyry (Izawa, 1981). Sugaki et al. (1981) identified two mineralization stages of the Maruyama deposit of the Tsumo mine with an early-stage mineralization accompanying skarn formation and a later stage one characterized by quartz veins and concluded that the main Fe-oxide and Cu-, Fe-, Zn-, and Pb-sulfide ores belong to the former mineralization, and scheelite and some accessary sulfides to the latter mineralization. Based on the similarity of mineral assemblages and mineralization sequence between the Maruyama deposit of the Tsumo mine and the skarn deposit of the Yamato mine, Nagashima et al. (2016) summarized that the skarn deposits related to ilmenite-series granitoids in the San-yo and San-in districts are associated with minor later stage vein mineralization. In addition, Nagashima et al. (2016) suggested that the Naganobori copper skarn deposits share similar mineralogical characteristics with the Yamato skarn deposit.

In the present study, we investigate in detail the occurrences and chemical compositions of the ore and skarn minerals from the Eboshi deposit of the Naganobori mine, the largest among sixteen deposits in the Naganobori mining district, in order to clarify general and local characteristics of the skarn deposits in Akiyoshi Limestone Group. Special attention is paid to the cobalt-, bismuth-, silver-, and tellurium-bearing ore minerals in order to compare the ore minerals in the Eboshi deposit to those of the Yamato skarn deposit. The mineralization processes of the ore minerals are also discussed.

GEOLOGY AND ORE DEPOSITS OF THE NAGANOBORI COPPER MINE

The Akiyoshi Limestone Group in the Akiyoshi Plateau mainly consists of Carboniferous and Permian limestones (Ota, 1976). The ore deposits here are found at or near the contacts of the Hanano-yama granite porphyry and the Akiyoshi limestone (Fig. 1b). After Sasaki et al. (2014), the Hanano-yama granite porphyry shows oval shaped with a longer east to west diameter of ~ 800 m and a shorter north to south one of 300 m.

Sixteen principal skarn type deposits are distributed near to the Hanano-yama granite porphyry and its environs. Of those, the Imori, Eboshi, Hanano-yama, Hakujiki, Ogiri, and Oda deposits belong to the Naganobori copper mine of the time of development. The Imori deposit, formerly known as the Naganobori deposit, occurs along the bedding plane between the limestone and greenstone, and the others occur along the contact with limestone (Fig. 1b; e.g., Kato, 1916, Ikeda, 2015).

According to Kato (1916), the orebody in the Eboshi deposit occurs the contact of the granite-porphyry and limestone, as a large irregular mass, rudely tabular in form, of about 100 m long, 10 m width at the maximum, and the depth with more than 75 m (Fig. 1b). It elongates to a direction from west to east and has an inclination of about 65° towards to the south. The boundaries between the deposit and the wall rocks are commonly very sharply defined. The orebody consists mainly of hedenbergite and garnet skarns mingled with metallic ores. The occurrence and chemical compositions of the hedenbergite and garnet (andradite) skarns indicate that large quantities of iron and silica have been introduced from the consolidating granite-porphyry magma to the limestone, and that the main deposit or the skarn mass has been formed by a process of metasomatism. The hedenbergite skarn is the chief gangue, and moderate quantities of garnet skarn is closely associated with hedenbergite skarn. Although the hedenbergite skarn and garnet skarn show some minor and fortuitous relations, and comparative abundance of the garnet skarn higher in the upper part of the deposit than the lower part, the garnet skarn is generally very irregularly distributed in the hedenbergite, indication that both skarns were formed in the same stage of mineralization. Though wollastonite occurs as a minor skarn mineral, it has been formed at the earliest epoch of the contact metasomatism, which is proved by the fact that the wollastonite mass is frequently traversed by veinlets of garnet, of hedenbergite or of a mixture of these minerals with sulfide minerals. Kato (1916) also noted that the garnet skarn always incorporates small irregular masses of magnetite, and that the main skarns are cut by veins and veinlets of cobaltite-quartz mass.

The ore minerals described by Kato (1916) are chalcopyrite, bornite, tetrahedrite, cobaltite, magnetite, pyrite, pyrrhotite, arsenopyrite, native bismuth, bismuthinite, native silver, hematite and scheelite, and the gangue minerals hedenbergite, garnet, calcite, wollastonite, fluorite, and ilvaite. In oxidized ore, limonite, chrysocolla, black cobalt oxide, malachite, cuprite, azurite, erythrite, chalcophyllite, and olivenite were also reported. The cobaltite has been reported only from the Eboshi and the Imori deposits. Black cobalt oxide reported by Kato (1916) may correspond to heterogenite described by Nambu et al. (1970).

SPECIMENS

The specimens studied here were collected from the mine dump of the Eboshi deposit. The specimens are one massive magnetite ore, and thirty copper ores associated with skarns.

Skarns are categorized as clinopyroxene skarn, garnet skarn, and wollastonite skarn, and the clinopyroxene skarn is the most dominant. The clinopyroxene skarn is rich in hedenbergite with euhedral to subhedral prismatic crystals (max. 3.5 cm long), and dark green in color. The garnet skarn is mainly composed of euhedral to subhedral pale greenish yellow andradite crystals (0.5–2 mm in size). The wollastonite skarn is characterized by radial aggregates of wollastonite.

Selected samples are as follows: the magnetite massive ore (labeled as Ebs-Mag01); copper ores of Ebs-Hd01, 02, and 03 in the clinopyroxene skarn; a copper ore of Ebs-Grt01 in the garnet skarn; and a copper ore of Ebs-Wo01 in the wollastonite skarn. A main and common ore mineral in the copper ores is chalcopyrite. In some specimens, secondary green malachite fills in the fractures and occurs botryoidally on the surface of the sample Ebs-Hd02. On the surface of the sample Ebs-Hd03, erythrite with purplish pink in color occur botryoidally.

ANALYTICAL METHOD

Chemical analyses of minerals were made using a JEOL JXA8230 electron microprobe analyzer (EMPA) installed at the Centre for Instrumental Analysis, Yamaguchi University. The operating conditions used were an accelerating voltage of 20 kV for sulfides and 15 kV for silicates and oxides, beam current of 20 nA, and beam diameter of 1–10 μm. Wavelength-dispersion spectra were collected using LiF, PET, and TAP monochromator crystals to identify interfering elements and to locate the best wavelengths for background measurements. Abundances of S, Se, Ag, Pb, Sb, Cu, Ti, Cr, Fe, V, Zn, Cd, As, Mn, Bi, Au, Ni, Co, W, Y, P, Si, Al, Sn, Ca, In, Mg, K, and Mo were determined for sulfides, and Si, Ti, Al, Cr, V, Fe, Mn, Mg, Ca, Sr, Ba, Na, K, Ni, Pb, Cd, Zn, S, As, P, Ag, W, and Sn for all others. The probe standards used were: metals for gold (Au$L\alpha$), silver (Ag$L\alpha$), copper (Cu$K\alpha$), molybdenum (Mo$L\alpha$), and InSb (In$L\alpha$, Sb$L\alpha$), natural mineral standards of pyrite (S$K\alpha$, Fe$K\alpha$), sphalerite (S$K\alpha$, Zn$K\alpha$), hematite (Fe$K\alpha$), wollastonite (Si$K\alpha$, Ca$K\alpha$), cassiterite (Sn$L\alpha$), K-feldspar (Si$K\alpha$, K$K\alpha$), and albite (Si$K\alpha$, Na$K\alpha$), and synthetic standards of eskolaite (Cr$K\alpha$), $Ca_3(VO_4)_2$ (V$K\alpha$), ZnO (Zn$K\alpha$), CdSe (Cd$L\alpha$, Se$L\alpha$), GaAs (As$L\alpha$), manganosite (Mn$K\alpha$), $Bi_4Ge_3O_{12}$ (Bi$M\alpha$), NiO (Ni$K\alpha$), CoO (Co$K\alpha$), scheelite (W$L\alpha$), $(Zr, Y)O_2$ (Y$L\alpha$), $KTiOPO_4$ (P$K\alpha$, K$K\alpha$), PbVGe-oxide (Pb$M\alpha$, V$K\alpha$), rutile (Ti$K\alpha$), corundum (Al$K\alpha$), periclase (Mg$K\alpha$), and $SrBaNb_4O_{12}$ (Sr$L\alpha$, Ba$L\alpha$). Overlaps of characteristic spectra due to nearby wavelengths were corrected using JEOL software. The ZAF method was used for data correction.

PETROGRAPHY OF ORES AND SKARNS

Ores

Mineral assemblages of the massive ore and skarn ore samples are listed in Table 1. The massive magnetite ore (Ebs-Mag01) consists of mainly anhedral magnetite grains, generally >200 μm in size (Fig. 2). Chalcocite, bornite, chalcopyrite and idaite fill the fractures in the magnetite grains. Cuprite also occurs as minor inclusions. A part of magnetite is altered to goethite (Fig. 2).

In the ores occurring in clinopyroxene skarn, pyrite, chalcopyrite, and cobaltite are common ore minerals (Fig. 3). Chalcopyrite is the most abundant among them. Sphalerite and pyrrhotite are associated with chalcopyrite (Fig. 3a). Bornite is rather minor. It is associated with chalcopyrite and sphalerite (Fig. 3b), but it commonly occurs as replacement of chalcopyrite (Fig. 3c). Pyrite was observed in clinopyroxene skarn, but not in the garnet and wollastonite skarns. Pyrite occurs as euhedral to subhedral crystals with 50–200 μm in size. It often forms aggregates with cobaltite crystals (Fig. 3d) and grows on cobaltite (Fig. 3e). Backscattered electron image of pyrite in Figure 3e indicates that there are at least two generations of pyrite. Hereafter, early generation and later generation pyrites are referred to as Py-I and Py-II, respectively. In the ore specimen Ebs-Hd03 of which surface is covered with erythrite, cobaltite is the most abundant ore mineral instead of chalcopyrite. Chalcopyrite is commonly associated with cobaltite (Fig. 3f). As well, it characteristically occurs as inclusions or fillings within cobaltite and fillings of interstices in cobaltite ± pyrite (Py-I and Py-II) aggregates (Figs. 3d and 3e); and as overgrowth on cobaltite. Euhedral to subhedral cobaltite shows oscillatory zoning indicated by Co ↔ Fe substitution (Fig. 3g). Sphalerite also occurs along with chalcopyrite within the open space in the aggregates of pyrite and cobaltite (Fig. 3e). Cassiterite and bismuthinite occur on the rim of chalcopyrite (Fig. 3c). Cassiterite occurs as euhedral to subhedral prismatic crystals (Figs. 3c and 3h). Various later stage ore minerals occur within the cavities in the earlier stage minerals described above and within the interstices in their aggregates: in the cavities of the host ore minerals, native bismuth (Fig. 3i), bismuthinite (Fig. 3j), skutterudite (Fig. 3k) and safflorite occur; and, within the in-

Table 1. Mineral assemblages of ores of the Eboshi deposit, the Naganobori copper skarn deposit[1)]

Skarn type	Simplified formula	Massive ore	Clinopyroxene skarn			Garnet skarn	Wollastonite skarn	Kato (1916)
Sample name		Ebs-Mag01	Ebs-Hd01	Ebs-Hd02	Ebs-Hd03	Ebs-Grt01	Ebs-Wo01	
Ore minerals								
Magnetite	$Fe^{2+}Fe^{3+}{}_2O_4$	+++						+
Pyrite	FeS_2		+	+	++			+
Pyrrhotite	FeS				+			+
Chalcopyrite	$CuFeS_2$	-	++	++	++	++	+	+++
Bornite	Cu_5FeS_4	+	++	++		++	+	+++
Idaite	Cu_3FeS_4	-				-	-	
Covellite	CuS					+	+	
Chalcocite	Cu_2S	+					+	
Sphalerite	(Zn, Fe)S			-	+		-	
Cobaltite	CoAsS		++	+	++			+
Skutterudite	$(Co, Ni)As_{3-x}$			-	-			
Safflorite	$CoAs_2$			-	-			
Native bismuth	Bi		+	+	+			-
Bismuthinite	Bi_2S_3		+	-	+			+
Emplectite	$CuBiS_2$			+				
Wittichenite	Cu_3BiS_3		+	+		-	-	
Ag-bearing cuprobismutite	$Cu_{10}Bi_{12}S_{23}$			-				
Matildite	$AgBiS_2$		-					
Kawazulite	$Bi_2(Te, Se, S)_3$			-				
Tsumoite	BiTe					-		
Sulphotsumoite	$BiTe_2S$			-				
Joséite-A	Bi_4TeS_2			-	-			
Hessite	Ag_2Te						-	
Arsenopyrite	FeAsS							+
Tetrahedrite	$(Cu, Fe)_{12}Sb_4S_{13}$							+
Native silver	Ag							-
Hematite	Fe_2O_3			+				-
Cassiterite	SnO_2		+	-	+	+		
Scheelite	$CaWO_4$		+	-		+		+

[1)] Abundance: +++ (abundant) > ++ (common) > + (minor) > − (rare)
[2)] 'Cuprotrichite' is not a mineral name but a collective term indicating the hair-like crystallite.

terstices in the aggregates of early stage minerals, hematite (Figs. 3l and 3m), kawazulite (Fig. 3m), wittichenite, emplectite (Fig. 3n), Ag-bearing cuprobismutite (Figs. 3h and 3k), tsumoite, joséite-A and matildite (Fig. 3o) occur. Wittichenite is commonly associated with emplectite (Fig. 3n), and sometimes with Ag-bearing cuprobismutite. Kawazulite rarely occurs on the rim of bismuthinite (Fig. 3m). Native bismuth is formed on the rim of bismuthinite. Unidentified Bi-Cu-bearing hydrous sulfate rarely occurs on the rim of bismuthinite (Fig. 3m). Malachite and erythrite occur on the surface of the Cu ores and a cobaltite-rich ore (Ebs-Hd03).

In the garnet skarn, andradite is associated with clinopyroxene and quartz (Fig. 4a), and chalcopyrite is the predominant ore mineral (Fig. 4b). Bornite and idaite are associated with chalcopyrite. Covellite is crystallized on the surface of the ore samples. Short prismatic cassiterite crystals, wittichenite, and tsumoite grains are found within the interstices in the aggregates of calcite and chalcopyrite.

In the wollastonite skarn (Fig. 5a; Ebs-Wo01), chalcopyrite and bornite are the dominant ore minerals of the Cu ore (Fig. 5b). Idaite is associated with bornite. Wittichenite rarely presents in interstices of bornite. Chalcocite occurs in calcite or at the boundary between the aggregates of wollastonite and calcite in marble (Fig. 5b). Cov-

Table 1. (Continued)

Skarn type	Simplified formula	Massive ore	Clinopyroxene skarn			Garnet skarn	Wollastonite skarn	Kato (1916)
Sample name		Ebs-Mag01	Ebs-Hd01	Ebs-Hd02	Ebs-Hd03	Ebs-Grt01	Ebs-Wo01	
Gangue minerals								
Skarn minerals								
Hedenbergite	$CaFeSi_2O_6$		+++	+++	+++	++	++	+++
Diopside	$CaMgSi_2O_6$		+			+	++	
Andradite	$Ca_3Fe^{3+}{}_2Si_3O_{12}$		+	+		+++	+	
Wollastonite	$CaSiO_3$						+++	+
Ilvaite	$CaFe^{2+}Fe^{3+}{}_2Si_2O_8(OH)$		++	++		+	+	-
Babingtonite	$Ca_2Fe^{2+}Fe^{3+}Si_5O_{14}(OH)$			+				
Other minerals								
Quartz	SiO_2		+	+	++	+	+	+
Fluorite	CaF_2		+					+
Calcite	$CaCO_3$		+	+	++	+	+++	++
Fluorapatite	$Ca_5(PO_4)_3F$						+	
Plagioclase	$(Na, Ca)(Al, Si)_4O_8$		+			+	+	
Chlorite-group minerals	$(Mg, Fe)_5Al(Si_3Al)O_{10}(OH)_8$		-	+	+	+		
Fluorapophyllite-(K)	$KCa_4Si_8O_{20}F \cdot 8H_2O$						+	
Secondary minerals								
Erythrite	$Co_3(AsO_4)_2 \cdot 8H_2O$				++			-
Malachite	$Cu(OH)_2CO_3$			++	-	+		+
Azurite	$Cu_3(OH)_2(CO_3)_2$				-			-
Cuprite	Cu_2O	+		+				+
Shattuckite	$Cu_5(SiO_3)_4(OH)_2$			+				
Goethite	$Fe^{3+}O(OH)$	++	+	++		+		
Sillenite	$Bi_{12}SiO_{20}$			+				
Daubréeite	$BiO(OH, Cl)$			+				
Bismutoferrite	$BiFe^{3+}{}_2(SiO_4)_2(OH)$			+				
Crednerite	$CuMnO_2$			+				
Chrysocolla	$CuSiO_3 \cdot 2H_2O$							+++
Olivenite	$Cu_2AsO_4(OH)$							-
Chalcophyllite	$Cu_{18}Al_2(AsO_4)_4(SO_4)_3(OH)_2$							-
Limonite	$FeO(OH) \cdot n\,H_2O$							+++
Black cobalt oxide								+
Cuprotrichite[2)]								-

[1)] Abundance: +++ (abundant) > ++ (common) > + (minor) > − (rare)
[2)] 'Cuprotrichite' is not a mineral name but a collective term indicating the hair-like crystallite.

ellite is associated with chalcocite. Sphalerite is found in interstices of calcite. Tiny hessite grains are observed in clinopyroxene (Fig. 5b). Fluorapophyllite-(K) closely associated with calcite and clinopyroxene are presented in Figure 5c.

Skarns

Hedenbergite is the most abundant skarn mineral in specimen Ebs-Hd01, 02, and 03, which is partly chloritized. Minor garnet and ilvaite occur occasionally in specimens Ebs-Hd01 and 02, whereas they are absent in Ebs-Hd03. Babingtonite occurs in Ebs-Hd02. The occurrence of hedenbergite, ilvaite, and babingtonite in Ebs-Hd02 is shown in Figure 3l. Calcite and quartz are the major gangue minerals in all clinopyroxene skarn specimens. In addition, fluorite and plagioclase are found in Ebs-Hd01.

Garnet is the main constituent of garnet skarn, Ebs-Grt01. Optical anomalies are not observed. Garnet is surrounded by quartz and calcite, which also infill fractures

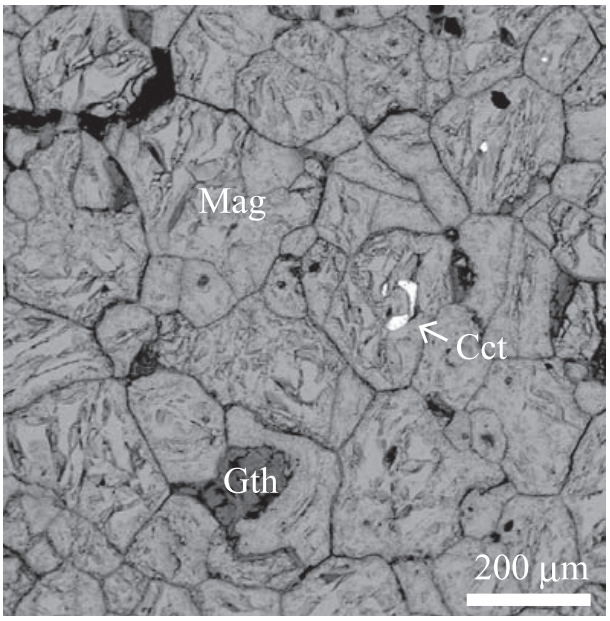

Figure 2. Back-scattered electron image of massive ore, Ebs-Mag01. Mineral abbreviations: Mag, magnetite; Gth, goethite; Cct, chalcocite.

within quartz and calcite. Clinopyroxene, ilvaite, and secondary goethite also fill the fractures in garnet grains (Fig. 4a).

Wollastonite occurs as radiating aggregates in the wollastonite skarn specimen, Ebs-Wo01 (Figs. 5a and 5b). Matrix is composed of calcite, fluorapophyllite-(K), and quartz (Figs. 5b and 5c). Small fragments of clinopyroxene, garnet, and ilvaite were also found in Ebs-Wo01, which occur interstices of the radiating wollastonite aggregates or are surrounded by calcite or quartz. Anhedral coarse clinopyroxene grains occur on the boundary between wollastonite skarn and marble, which is associated with chalcocite (Fig. 5c).

MINERAL CHEMISTRY

The chemical compositions of the characteristic ore minerals of the ores are listed in Table 2, and those of the skarn minerals are in Table 3.

Ore minerals

Common ore minerals. Pyrites of Py-I and Py-II in the ores occurring in the clinopyroxene skarn (Fig. 3e) are As-poor and As-rich ones, respectively. The As content in the Py-II attains up to 5.19 wt% As (Table 2), which gives the formulae $Fe_{1.01}(S_{1.91}As_{0.09})$. The chemical formula of pyrrhotite is represented as $Fe_{0.86}S$ (Table 2). Average chemical compositions of sphalerite in the ores occurring in the clinopyroxene skarn and wollastonite skarn are $(Zn_{0.84}Fe_{0.13}Cd_{0.01}Cu_{0.01})_{\Sigma 0.99}S$ (n = 7) and $(Zn_{0.87}Fe_{0.11}Cd_{0.01})_{\Sigma 0.99}S$ (n = 2), respectively (Table 2). Cassiterite and scheelite have almost ideal compositions, SnO_2 and $CaWO_4$, respectively.

Cu-Fe- and Cu-sulfides. Chalcopyrite is homogeneous (Figs. 3c and 4b) and almost ideal in composition (Table 2). Bornite in the Cu ores except for the garnet skarn is also homogeneous (Figs. 3b and 3c) and close to the ideal composition, whereas very small amount of Ag (0.26 wt% Ag in average) was detected in bornite from the Cu ore occurring in the garnet skarn (Table 2). Idaite is mostly too small for EMPA analysis, but one available EMPA data gives the chemical formula of $Cu_{3.02}Fe_{0.99}(S_{3.99}Se_{0.01})$ on a basis of S + Se = 4 (Table 2). Covellite in the ore with garnet skarn contains 0.60 wt% Ag and is of the formula of $(Cu_{0.96}Fe_{0.04}Ag_{0.01})_{\Sigma 1.01}S$ (Table 2). Chalcocite in the massive ore (Fig. 2) and in the ore with the wollastonite skarn has chemical compositions represented by the formulae $(Cu_{1.88}Fe_{0.16})_{\Sigma 2.04}S$ and $(Cu_{1.98}Fe_{0.01})_{\Sigma 1.99}S$, respectively.

Co-As-bearing sulfides. Average chemical formula of cobaltite is $(Co_{0.96}Fe_{0.04})_{\Sigma 1.00}As_{0.97}(S_{0.99}Se_{0.01})$ (n = 63) (Table 2). Cobaltite in the ores with the clinopyroxene skarn contains Fe and Ni of 2.78 and 0.21 wt% at maximum, respectively. Most of cobaltite is homogeneous in chemical composition, but some grains show the chemical variation due to Co ↔ Fe substitution (Fig. 3g). The chemical formulae of skutterudite and safflorite are represented as $(Co_{0.97}Fe_{0.03})_{\Sigma 1.00}(As_{2.81}S_{0.03}Se_{0.02})_{\Sigma 2.86}$ (n = 4) and

Figure 3. Photographs of the ores of the hedenbergite skarn. (a), (b), (f), (h), and (j)-(o) Ebs-Hd02. (d), (e), (g), and (i) Ebs-Hd03. (c) Ebs-Hd01. (a) Reflected light photomicrograph of chalcopyrite (Ccp), sphalerite (Sp), and pyrrhotite (Po). (b) Reflected light photomicrograph of Ccp, Sp, and bornite (Bn). (c) Back-scattered electron (BSE) image of Ccp, Bn, bismuthinite (Bmt), cassiterite (Cst), goethite (Gth), hedenbergite (Hd), and quartz (Qz). (d) Reflected light photomicrograph of cobaltite (Cbt), pyrite (Py), and Ccp. (e) BSE image and element concentration maps (As and S) of pyrite-I (Py-I), pyrite-II (Py-II), Ccp, Cbt, and Sp. (f) Occurrence of Cbt, Ccp, and malachite (Mlc) in the hand specimen. (g) BSE image and element concentration maps (Co and Fe) of Cbt. (h) BSE image of Ag-bearing cuprobismutite (Ag-Cbm), Cbt, native bismuth (Bi), and Cst. (i) BSE image of Cbt, Py-I, Py-II, Ccp, and Bi. (j) Reflected light photomicrograph and BSE image of Bi, Bmt, Cbt, Ccp, and calcite (Cal). (k) BSE image of Ag-Cbm, Cbt, and skutterudite (Skt). (l) BSE image of the association of Ca-Fe-silicate minerals such as babingtonite (Bab), ilvaite (Ilv) and Hd with Cbt, hematite (Hm), and Qz. (m) BSE image and element concentration maps (Bi and Te) of Bmt, Bi, kawazulite (Kwz), Ccp, Hem, and Ilv. (n) BSE image of emplectite (Emp), wittichenite (Wcn), Ccp, and Cbt. (o) BSE image of Cal, Hd, and matildite (Mtd).

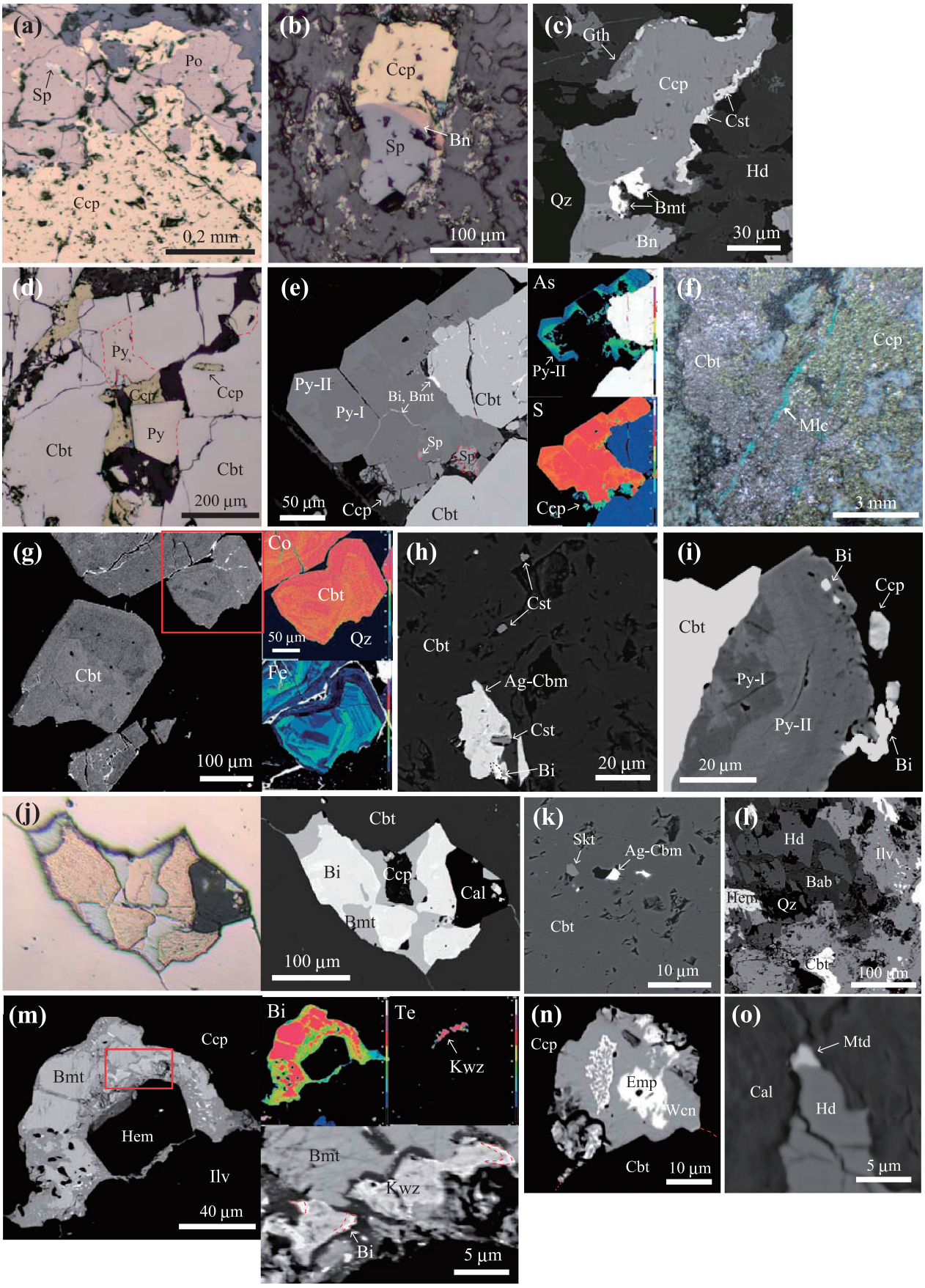
(a)
Po
Sp
Ccp
0.2 mm
(b)
Ccp
Sp
Bn
100 µm
(c)
Gth
Ccp
Cst
Hd
Qz
Bmt
Bn
30 µm
(d)
Py
Ccp
Ccp
Py
Cbt
Cbt
200 µm
(e)
Py-II
Bi, Bmt
Py-I
Cbt
Sp
Sp
50 µm
Ccp
Cbt
As
Py-II
S
Ccp
(f)
Ccp
Cbt
Mlc
3 mm
(g)
Cbt
100 µm
Co
Cbt
50 µm
Qz
Fe
(h)
Cst
Cbt
Ag-Cbm
Cst
Bi
20 µm
(i)
Bi
Ccp
Cbt
Py-I
Py-II
20 µm
Bi
(j)
Cbt
Bi
Ccp
Cal
Bmt
100 µm
(k)
Skt
Ag-Cbm
Cbt
10 µm
(l)
Hd
Ilv
Bab
Hem
Qz
Cbt
100 µm
(m)
Ccp
Bmt
Hem
Ilv
40 µm
Bi
Te
Kwz
Bmt
Kwz
Bi
5 µm
(n)
Ccp
Emp
Wcn
Cbt
10 µm
(o)
Mtd
Cal
Hd
5 µm

$(Co_{0.59}Fe_{0.40})_{\Sigma 0.99}(As_{1.86}S_{0.12}Se_{0.02})$ (n = 3), respectively (Table 2).

Bi-, Bi-Cu-, Bi-Ag-, Bi-Te-, and Ag-Te-minerals. Native bismuth in the ores with clinopyroxene skarn is pure. Bismuthinite in the ores with clinopyroxene skarn is $(Bi_{1.97}Cu_{0.02})_{\Sigma 1.99}(S_{2.98}Se_{0.02})$ in average chemical formula (n = 26) (Table 2). Wittichenite and emplectite in the ores with clinopyroxene skarn have the average formulae of $(Cu_{2.92}Ag_{0.07}Fe_{0.01})_{\Sigma 3.00}Bi_{1.00}(S_{2.98}Se_{0.02})$ (n = 14) and $(Cu_{0.96}Fe_{0.02}Ag_{0.02})_{\Sigma 1.00}Bi_{1.00}(S_{1.99}Se_{0.01})$ (n = 6), respectively. The Ag content attains 3.61 wt% in wittichenite and 3.60 wt% in emplectite, respectively. Ag-bearing cuprobismutite has the average formula of $(Cu_{7.79}Ag_{2.18}Fe_{0.37}Cd_{0.02}Pb_{0.01}Bi_{11.61})_{\Sigma 21.98}(S_{22.86}Se_{0.12}Te_{0.03})$ (n = 8) (Table 2) with maximum Ag content of 6.47 wt%. Fine matildite grain occurring on the rim of calcite (Fig. 3o) has a formula $(Ag_{0.97}Cu_{0.01})_{\Sigma 0.98}Bi_{0.99}(S_{1.91}Se_{0.07}Te_{0.02})$ (Table 2). Some tellurium-bearing phases rarely occur. Kawazulite in a Cu ore, Ebs-Hd02 (Fig. 3m), has the average chemical formula of $(Bi_{1.87}Fe_{0.05}Cu_{0.05}Ag_{0.03}Sb_{0.01})_{\Sigma 2.01}(Te_{1.80}S_{1.12}Se_{0.07})$ (n = 3) (Table 2). Tsumoite in the ore, Ebs-Grt01, with garnet skarn has a formula $(Bi_{0.92}Co_{0.04}Fe_{0.04}Pb_{0.02})_{\Sigma 1.02}(Te_{0.97}S_{0.03})$ (Table 2), where Co and Fe may be attributed to the cobaltite surrounding tsumoite. The chemical formulae of sulphotsumoite and joséite-A are represented as $(Bi_{2.72}Fe_{0.04}Cu_{0.17}Sb_{0.01})_{\Sigma 2.94}(Te_{1.95}S_{1.01}Se_{0.04})$ (Table 2) and $(Bi_{3.90}Fe_{0.09}Cu_{0.02})_{\Sigma 4.01}(S_{1.98}Te_{0.94}Se_{0.08})$ (n = 3) (Table 2), respectively, where small amounts of Cu and Fe are possibly due to host chalcopyrite. Hessite occurring on the rim of clinopyroxene in the wollastonite skarn (Ebs-Wo01) (Fig. 5b) has a formula $(Ag_{2.00}Cu_{0.01}Fe_{0.01})_{\Sigma 2.02}(Te_{0.98}S_{0.02})$ (Table 2). Unidentified silver-concentrated phases with 72 wt% Ag at maximum are observed in the ore specimens. They seem to be weathered product from the Ag-rich ore minerals.

Skarn minerals

Clinopyroxene. The clinopyroxene in the clinopyroxene skarn (Ebs-Hd01 and 02) is hedenbergite with chemical compositions in a range between $Hd_{98.2}Jo_{1.8}$ and $Hd_{76.3}Di_{16.9}Jo_{6.8}$ with an average of $Hd_{89.9}Jo_{5.9}Di_{4.2}$ (n = 56), where Hd, Jo, and Di represent $CaFe^{2+}Si_2O_6$ (hedenbergite), $CaMn^{2+}Si_2O_6$ (johannsenite), and $CaMgSi_2O_6$ (diopside) components, respectively (Table 3 and Fig. 6a). Clinopyroxene in the garnet skarn is hedenbergite or diopside with $Hd_{97.7\text{-}22.9}Di_{1.2\text{-}76.3}Jo_{0.8\text{-}8.5}$ (n = 19) in composition. Clinopyroxene found interstices of wollastonite aggregates or along with quartz and/or calcite in the wollastonite skarn (Ebs-Wo01) is hedenbergite with compositions of $Hd_{94.8\text{-}73.2}Jo_{3.7\text{-}11.6}Di_{0.1\text{-}16.7}$ with an average of $Hd_{89.4}Jo_{6.0}Di_{4.6}$ (n = 18) (Cpx I in Table 3). Clinopyroxene occurring on the boundary between wollastonite skarn and marble (Fig. 5c) and in the fractures has Mg-rich core and Fe-rich rim, and of significantly variable chemical composition of $Hd_{86.4\text{-}7.5}Di_{9.2\text{-}92.2}Jo_{0.3\text{-}33.8}$ (n = 25) (Cpx II in Table 3 and Fig. 6a). The MnO content tends to be higher in the Fe-rich rim and reaches 9.94 wt% (Fig. 6a).

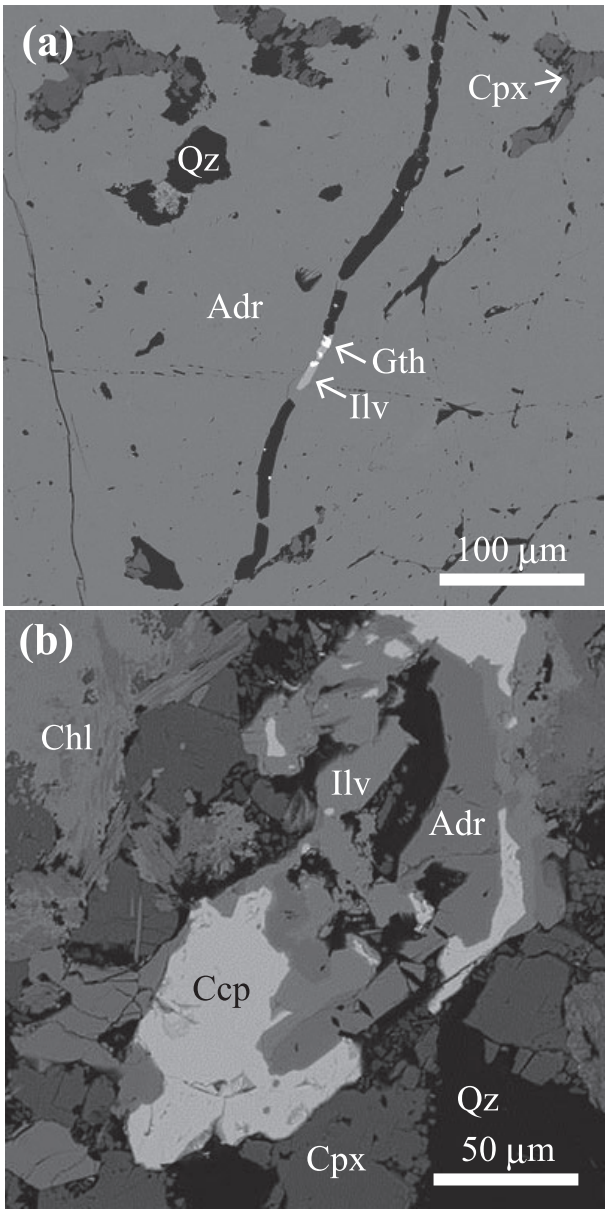

Figure 4. BSE images of the ore of the garnet skarn (Ebs-Grt01). (a) Andradite (Adr) with quartz (Qz), and clinopyroxene (Cpx) in the interstices of goethite (Gth) and ilvaite (Ilv). (b) Chalcopyrite (Ccp) with Adr, Ilv, Qz, Cpx, and chlorite (Chl).

Garnet. Garnet in all skarn types is andradite (Fig. 6b) with the chemical composition of $Adr_{99.4\text{-}94.2}Grs_{0.0\text{-}5.6}Sps_{0.0\text{-}0.5}Pyp_{0.0\text{-}0.8}$ in the garnet skarn (n = 14 in Table 3) and $Adr_{99.6\text{-}92.0}Grs_{0.0\text{-}7.3}Sps_{0.2\text{-}1.8}Pyp_{0.0\text{-}0.4}$ (n = 15 in Table 3) in the wollastonite skarn, where Adr, Grs, Sps, and Prp

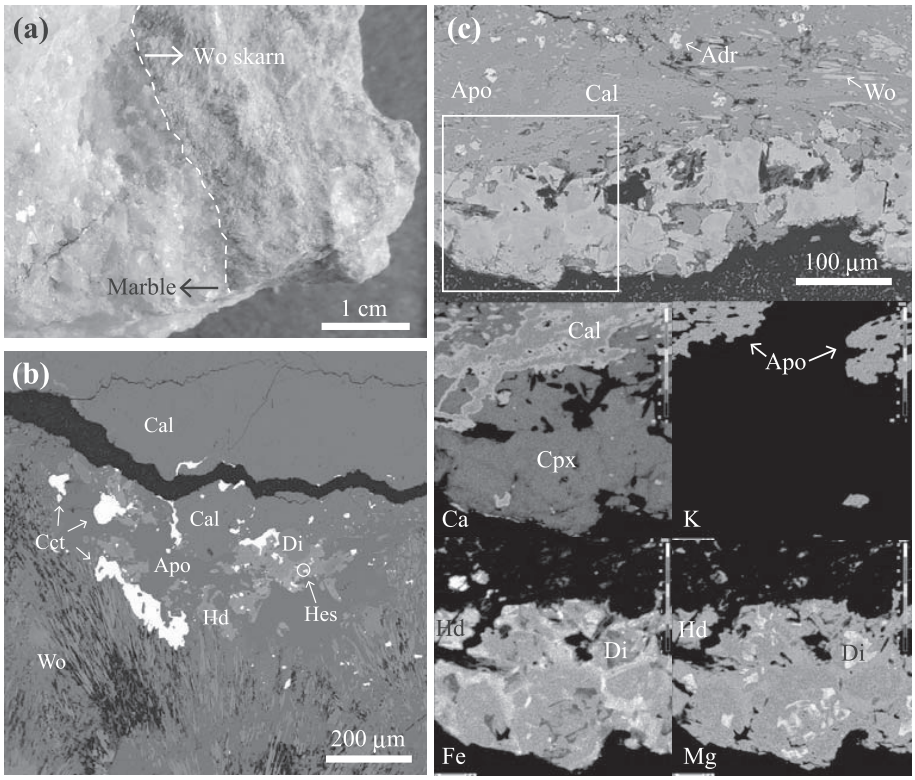

Figure 5. Photographs of the ore of the wollastonite skarn (Ebs-Wo01). (a) Boundary between marble and wollastonite skarn in the hand specimen. (b) BSE image of wollastonite (Wo), hedenbergite (Hd), diopside (Di), calcite (Cal), chalcocite (Cct), and hessite (Hes). (c) BSE image of fluorapophyllite-(K) (Apo), calcite (Cal), andradite (Adr), and Wo and element concentration maps (Ca, K, Fe, and Mg) of fluorapophyllite-(K), Cal, and clinopyroxene (Cpx) including Hd and Di. Color version is available online from https://doi.org/10.2465/jmps.200818.

represent $Ca_3Fe^{3+}_2Si_3O_{12}$ (andradite), $Ca_3Al_2Si_3O_{12}$ (grossular), $Mn^{2+}_3Al_2Si_3O_{12}$ (spessartine), and $Mg_3Al_2Si_3O_{12}$ (pyrope) components, respectively. Garnet in the clinopyroxene skarn has composition of $Adr_{99.5}Grs_{0.3}Sps_{0.1}Prp_{0.1}$, close to Adr end-member composition (Table 3).

Other skarn minerals. Wollastonite in the wollastonite skarn has average formula of $(Ca_{0.86}Fe^{2+}_{0.11}Mn^{2+}_{0.02})_{\Sigma 0.99}Si_{1.00}O_3$ (n = 13) (Table 3). The FeO and MnO contents attain up to 9.5 and 1.7 wt%, respectively. Ilvaite in the clinopyroxene skarn is $Ca_{1.00}(Fe^{2+}_{1.86}Mn_{0.13})_{\Sigma 1.99}(Fe^{3+}_{1.01}Al_{0.01})_{\Sigma 1.02}Si_{1.99}O_8(OH)$ (n = 53) in chemical formula (Table 3). Chemical composition of ilvaite in each skarn is similar to each other (Table 3), and Fe^{2+}/total Fe in ilvaite in three types of skarns, estimated based on electronic neutralization, is 0.65. The MnO content in ilvaite attains 4.10 wt% in the clinopyroxene skarn, 5.25 wt% in the garnet skarn and 3.42 wt% in the wollastonite skarn. Babingtonite in Ebs-Hd02 is $Ca_{2.00}(Fe^{2+}_{0.76}Mn^{2+}_{0.20}Mg_{0.04})_{\Sigma 1.00}(Fe^{3+}_{0.98}Al_{0.02})_{\Sigma 1.00}Si_{5.00}O_{14}(OH)$ (n = 3) in average formula (Table 3). Fe^{2+}/total Fe in is 0.44.

DISCUSSION

Mineralization sequence of ore minerals

Based on the occurrences of skarns and ores and their textural relations, Kato (1916) recognized four stages of mineralization in the formation of the Eboshi skarn deposit as follows; (1) the first stage of mineralization characterized by wollastonitization; (2) the second stage of mineralization is of formation of principle skarns, or the main ore deposit, at which succession of mineral depositions scheelite, ilvaite, hedenbergite, magnetite, andradite, various sulfides such as pyrite, arsenopyrite, pyrrhotite, and chalcopyrite, quartz, calcite and fluorite; (3) the third stage of mineralization is the stage of the formation of cobaltite-quartz veins, often accompanied by bismuth ores consisting of native bismuth and bismuthinite; (4) the fourth stage of mineralization is the stage of the formation of chalcopyrite veins and veinlets, and the larger part of tetrahedrite is of deposition at this stage.

In this study, we recognized four ore mineralization stages, represented as stages I, II, III, and IV in Figure 7, corresponding to the second, third, and fourth mineralization stages defined by Kato (1916). The mineralization stage I in this study is characterized by the crystallization of the main ore minerals, such as chalcopyrite, bornite, pyrrhotite, sphalerite, and pyrite-I, which fill the cracks and interstices of individual clinopyroxene and garnet grains, indicating that major skarn minerals are obviously crystallized before the main ore minerals. The stage II in this study is defined by the mineralization of cobaltite, pyrite-II, and Bi(-Cu)-bearing sulfides, such as native bismuth, bismuthinite, and wittichenite: bismuthinite oc-

Table 2. Chemical compositions of selected ore minerals

Skarn type[1)]	Cpx skarn			Cpx skarn	Cpx skarn	Wo skarn	Cpx skarn	Grt skarn
	Pyrite-I	Pyrite-II			Sphalerite		Chalcopyrite	
wt%	Ave. $n = 10$	Ave. $n = 17$	Max. As	Pyrrhotite	Ave. $n = 7$	Ave. $n = 2$	Ave. $n = 52$	Ave. $n = 9$
S	52.33	50.18	48.91	39.72	33.27	33.20	34.64	34.56
Se	0.03	0.08	0.07	0.00	0.03	0.11	0.07	0.10
Te	0.01	0.00	0.00	0.00	0.00	0.00	0.00	0.00
Ag	0.00	0.01	0.02	0.00	0.00	0.00	0.01	0.02
Pb	0.06	0.06	0.00	0.00	0.01	0.00	0.03	0.01
Sb	0.00	0.00	0.00	0.00	0.00	0.00	0.00	0.00
Cu	0.07	0.02	0.00	0.14	0.68	0.03	34.18	34.14
Ti	0.00	0.00	0.00	0.01	0.00	0.00	0.01	0.00
Cr	0.01	0.00	0.00	0.00	0.01	0.01	0.01	0.01
Fe	46.24	45.30	45.06	59.82	7.56	6.15	30.25	30.20
Zn	0.03	0.01	0.00	0.02	56.88	58.96	0.05	0.01
Cd	0.02	0.01	0.00	0.00	0.73	1.29	0.01	0.01
As	0.10	3.42	5.19	0.00	0.00	0.00	0.00	0.00
Mn	0.01	0.01	0.02	0.00	0.07	0.03	0.02	0.01
Bi	0.24	0.20	0.14	0.00	0.15	0.12	0.15	0.14
Ni	0.00	0.00	0.00	0.00	0.01	0.00	0.00	0.00
Co	0.15	0.14	0.11	0.00	0.13	0.02	0.18	0.05
W	0.01	0.01	0.02	0.00	0.03	0.00	0.02	0.00
Sn	0.01	0.00	0.00	0.00	0.00	0.00	0.01	0.02
In	0.03	0.00	0.00	0.00	0.04	0.00	0.01	0.00
Total	99.38	99.51	99.54	99.71	99.61	99.96	99.68	99.31
	S+Se+As = 2			S+Se = 1	S+Se = 1		S+Se = 2	
S	2.00	1.94	1.91	1.00	1.00	1.00	2.00	2.00
Se	0.00	0.00	0.00	0.00	0.00	0.00	0.00	0.00
Te	0.00	0.00	0.00	0.00	0.00	0.00	0.00	0.00
Ag	0.00	0.00	0.00	0.00	0.00	0.00	0.00	0.00
Pb	0.00	0.00	0.00	0.00	0.00	0.00	0.00	0.00
Sb	0.00	0.00	0.00	0.00	0.00	0.00	0.00	0.00
Cu	0.00	0.00	0.00	0.00	0.01	0.00	0.99	1.00
Ti	0.00	0.00	0.00	0.00	0.00	0.00	0.00	0.00
Cr	0.00	0.00	0.00	0.00	0.00	0.00	0.00	0.00
Fe	1.01	1.01	1.01	0.86	0.13	0.11	1.00	1.00
Zn	0.00	0.00	0.00	0.00	0.84	0.87	0.00	0.00
Cd	0.00	0.00	0.00	0.00	0.01	0.01	0.00	0.00
As	0.00	0.06	0.09	0.00	0.00	0.00	0.00	0.00
Mn	0.00	0.00	0.00	0.00	0.00	0.00	0.00	0.00
Bi	0.00	0.00	0.00	0.00	0.00	0.00	0.00	0.00
Ni	0.00	0.00	0.00	0.00	0.00	0.00	0.00	0.00
Co	0.00	0.00	0.00	0.00	0.00	0.00	0.01	0.00
W	0.00	0.00	0.00	0.00	0.00	0.00	0.00	0.00
Sn	0.00	0.00	0.00	0.00	0.00	0.00	0.00	0.00
In	0.00	0.00	0.00	0.00	0.00	0.00	0.00	0.00
Total	3.02	3.01	3.01	1.87	0.99	0.99	4.01	4.00

[1)] Cpx skarn, clinopyroxene skarn; Wo skarn, wollastonite skarn; Grt skarn, garnet skarn.

curs on the rim of chalcopyrite (Fig. 3c) and is associated with native bismuth in the cavity of cobaltite (Fig. 3j); wittichenite and emplectite occur as filling phases in the interstices between chalcopyrite and cobaltite grains (Fig. 3n); cassiterite occurs on the rim of chalcopyrite (Fig. 3c), within interstices in cobaltite, and as an inclusion in Ag-bearing cuprobismutite (Fig. 3h). Cassiterite and native bismuth are sometimes associated with ore minerals in this stage (Fig. 3h). The Ag- and/or Te-bearing ore minerals, such as matildite, kawazulite, tsumoite, and hessite, are the rather later stage minerals. This stage was defined as the mineralization stage III in this study. Kawazulite exists on the rim of bismuthinite (Fig. 3m); and Ag-bearing cuprobismutite occurs within the cavities in cobaltite grains (Figs. 3h and 3k). The stage IV in our study is characterized by chalcopyrite veins cutting

Table 2. (Continued-1)

Skarn type[1)]	Cpx skarn	Grt skarn	Wo skarn	Massive ore	Grt skarn	Grt skarn	Wo skarn	Massive ore
	Bornite				Idaite	Covellite	Chalcocite	
wt%	Ave. $n = 11$	Ave. $n = 4$	Ave. $n = 2$	Ave. $n = 5$		Ave. $n = 2$		Ave. $n = 2$
S	25.30	25.40	25.43	25.43	33.76	33.01	20.09	20.00
Se	0.14	0.09	0.14	0.00	0.15	0.07	0.14	0.00
Te	0.00	0.00	0.00	0.00	0.00	0.00	0.00	0.00
Ag	0.06	0.26	0.06	0.00	0.13	0.60	0.11	0.00
Pb	0.00	0.00	0.01	0.00	0.00	0.00	0.00	0.00
Sb	0.00	0.00	0.00	0.00	0.00	0.00	0.00	0.00
Cu	62.78	63.07	62.81	62.99	50.64	62.77	78.94	74.60
Ti	0.00	0.00	0.00	0.00	0.00	0.00	0.00	0.00
Cr	0.00	0.00	0.00	0.00	0.00	0.00	0.00	0.00
Fe	11.06	11.09	11.10	11.02	14.60	2.20	0.51	5.55
Zn	0.03	0.01	0.03	0.00	0.02	0.03	0.02	0.00
Cd	0.00	0.00	0.00	0.00	0.00	0.00	0.00	0.00
As	0.00	0.00	0.00	0.00	0.00	0.00	0.00	0.00
Mn	0.00	0.00	0.00	0.01	0.00	0.00	0.00	0.01
Bi	0.00	0.00	0.00	0.00	0.00	0.00	0.00	0.00
Ni	0.00	0.00	0.00	0.02	0.00	0.00	0.00	0.01
Co	0.02	0.02	0.00	0.00	0.01	0.02	0.01	0.00
W	0.00	0.00	0.00	0.00	0.00	0.00	0.00	0.00
Sn	0.00	0.00	0.01	0.00	0.00	0.00	0.00	0.00
In	0.00	0.00	0.00	0.00	0.00	0.00	0.00	0.00
Total	99.41	99.94	99.59	99.48	99.31	98.69	99.83	100.17
		S+Se = 4			S+Se = 4	S+Se = 1	S+Se = 1	
S	3.99	3.99	3.99	4.00	3.99	1.00	1.00	1.00
Se	0.01	0.01	0.01	0.00	0.01	0.00	0.00	0.00
Te	0.00	0.00	0.00	0.00	0.00	0.00	0.00	0.00
Ag	0.00	0.01	0.00	0.00	0.00	0.01	0.00	0.00
Pb	0.00	0.00	0.00	0.00	0.00	0.00	0.00	0.00
Sb	0.00	0.00	0.00	0.00	0.00	0.00	0.00	0.00
Cu	5.00	5.00	4.97	5.00	3.02	0.96	1.98	1.88
Ti	0.00	0.00	0.00	0.00	0.00	0.00	0.00	0.00
Cr	0.00	0.00	0.00	0.00	0.00	0.00	0.00	0.00
Fe	1.00	1.00	1.00	1.00	0.99	0.04	0.01	0.16
Zn	0.00	0.00	0.00	0.00	0.00	0.00	0.00	0.00
Cd	0.00	0.00	0.00	0.00	0.00	0.00	0.00	0.00
As	0.00	0.00	0.00	0.00	0.00	0.00	0.00	0.00
Mn	0.00	0.00	0.00	0.00	0.00	0.00	0.00	0.00
Bi	0.00	0.00	0.00	0.00	0.00	0.00	0.00	0.00
Ni	0.00	0.00	0.00	0.00	0.00	0.00	0.00	0.00
Co	0.00	0.00	0.00	0.00	0.00	0.00	0.00	0.00
W	0.00	0.00	0.00	0.00	0.00	0.00	0.00	0.00
Sn	0.00	0.00	0.00	0.00	0.00	0.00	0.00	0.00
In	0.00	0.00	0.00	0.00	0.00	0.00	0.00	0.00
Total	10.01	10.02	9.98	10.00	8.02	2.00	2.99	3.04

[1)] Cpx skarn, clinopyroxene skarn; Wo skarn, wollastonite skarn; Grt skarn, garnet skarn.

the main skarn masses and the host limestone and, thus, correspond to the fourth mineralization stage defined by Kato (1916).

Unfortunately, we do not have our own result for the mineralization stage of wollastonite skarn, because the studied samples consisting of wollastonite skarn is limited, and the relation between hedenbergite-garnet and wollastonite skarns is unclear. However, the direct contact between the limestone (marble) and wollastonite skarn ore observed in our studied specimen is consistent with the description by Kato (1916) that wollastonite is often found in irregular masses along the limestone. Because of the similar occurrence of wollastonite in our sample to that by Kato (1916), we agree the conclusion on the wollastonite skarn mineralization stage by Kato (1916) that the wollastonite skarn has been formed at

Table 2. (Continued-2)

Skarn type[1)]	Cpx skarn		Cpx skarn	Cpx skarn	Cpx skarn	Cpx skarn		Cpx skarn	
	Cobaltite		Skutterudite	Safflorite	Bismuthinite	Wittichenite		Emplectite	
wt%	Ave.	Range	Ave.	Ave.	Ave.	Ave.	Max.	Ave.	Max.
	n = 63		n = 4	n = 3	n = 26	n = 14	Ag	n = 6	Ag
S	19.23	18.01-20.24	0.30	1.93	18.67	19.02	19.10	18.77	18.62
Se	0.41	0.30-0.53	0.54	0.61	0.26	0.26	0.09	0.21	0.21
Te	0.01	0.00-0.03	0.01	0.00	0.00	0.00	0.00	0.07	0.14
Ag	0.01	0.00-0.03	0.00	0.01	0.01	1.59	3.61	0.68	3.60
Pb	0.04	0.00-0.16	0.04	0.04	0.11	0.00	0.00	0.00	0.00
Sb	0.00	0.00	0.00	0.00	0.01	0.00	0.00	0.00	0.00
Cu	0.02	0.00-0.53	0.05	0.01	0.25	36.84	36.03	17.97	15.51
Ti	0.00	0.00-0.03	0.00	0.00	0.01	0.01	0.00	0.00	0.00
Cr	0.00	0.00	0.00	0.00	0.00	0.00	0.00	0.00	0.00
Fe	1.39	0.43-2.78	0.71	11.01	0.02	0.06	0.00	0.37	0.79
Zn	0.00	0.00-0.02	0.00	0.00	0.00	0.01	0.00	0.00	0.00
Cd	0.01	0.00-0.04	0.01	0.02	0.00	0.00	0.02	0.03	0.20
As	43.98	43.09-45.12	77.51	68.39	0.01	0.00	0.00	0.00	0.00
Mn	0.01	0.00-0.05	0.00	0.01	0.02	0.01	0.00	0.00	0.02
Bi	0.11	0.02-1.76	0.04	0.15	80.21	41.50	41.07	61.30	61.04
Ni	0.07	0.01-0.21	0.04	0.03	0.01	0.01	0.00	0.00	0.00
Co	34.39	32.97-35.71	20.86	17.15	0.01	0.01	0.00	0.00	0.01
W	0.02	0.00-0.09	0.00	0.00	0.01	0.01	0.03	0.00	0.02
Sn	0.03	0.00-0.06	0.00	0.00	0.00	0.00	0.00	0.00	0.00
In	0.01	0.00-0.08	0.00	0.00	0.00	0.00	0.00	0.00	0.00
Total	99.78		100.11	99.38	99.65	99.34	99.95	99.47	100.25
	S+Se = 1		Co+Bi+Cu+Fe = 1	As+S+Se+Sb = 2	S+Se = 3	S+Se+Te = 3		S+Se+Te = 2	
S	0.99	0.99	0.03	0.12	2.98	2.98	2.99	1.99	1.99
Se	0.01	0.01	0.02	0.02	0.02	0.02	0.01	0.01	0.01
Te	0.00	0.00	0.00	0.00	0.00	0.00	0.00	0.00	0.00
Ag	0.00	0.00	0.00	0.00	0.00	0.07	0.17	0.02	0.11
Pb	0.00	0.00	0.00	0.00	0.00	0.00	0.00	0.00	0.00
Sb	0.00	0.00	0.00	0.00	0.00	0.00	0.00	0.00	0.00
Cu	0.00	0.00-0.01	0.00	0.00	0.02	2.92	2.85	0.96	0.84
Ti	0.00	0.00	0.00	0.00	0.00	0.00	0.00	0.00	0.00
Cr	0.00	0.00	0.00	0.00	0.00	0.00	0.00	0.00	0.00
Fe	0.04	0.01-0.08	0.03	0.40	0.00	0.01	0.00	0.02	0.05
Zn	0.00	0.00	0.00	0.00	0.00	0.00	0.00	0.00	0.00
Cd	0.00	0.00	0.00	0.00	0.00	0.00	0.00	0.00	0.01
As	0.97	0.91-1.04	2.81	1.86	0.00	0.00	0.00	0.00	0.00
Mn	0.00	0.00	0.00	0.00	0.00	0.00	0.00	0.00	0.00
Bi	0.00	0.00-0.01	0.00	0.00	1.97	1.00	0.99	1.00	1.00
Ni	0.00	0.00-0.01	0.00	0.00	0.00	0.00	0.00	0.00	0.00
Co	0.96	0.91-1.02	0.97	0.59	0.00	0.00	0.00	0.00	0.00
W	0.00	0.00	0.00	0.00	0.00	0.00	0.00	0.00	0.00
Sn	0.00	0.00	0.00	0.00	0.00	0.00	0.00	0.00	0.00
In	0.00	0.00	0.00	0.00	0.00	0.00	0.00	0.00	0.00
Total	1.98		3.86	3.00	2.00	4.00	4.01	2.00	2.01

[1)] Cpx skarn, clinopyroxene skarn; Wo skarn, wollastonite skarn; Grt skarn, garnet skarn.

the earliest epoch of the contact metasomatism. As already described, the matrix of the wollastonite skarn is composed of calcite, fluorapophyllite-(K), and quartz (Fig. 5c). We consider that fluorapophyllite-(K) associated with calcite does not belong to the first mineralization stage defined by Kato (1916), and that this mineral was formed by the metasomatic reaction between calcite and the solution containing fluorine and potassium, based on the suggestion for the fluorite formation by Kato (1916) that the fluorite was formed by the metasomatic reaction of F-bearing solutions on calcite. As well, such F-bearing solution might have produced fluorapophyllite-(K) (Table 4). Another interest is for coarse-grained diopside with ~ 92.2 mol% $CaMgSi_2O_6$ component occurring be-

Table 2. (Continued-3)

Skarn type[1)]	Cpx skarn		Cpx skarn	Cpx skarn	Grt skarn	Cpx skarn	Cpx skarn	Wo skarn
	Ag-bearing cuprobismutite		Matildite	Kawazulite	Tsumoite	Sulpho-tsumoite	Joséite-A	Hessite
wt%	Ave. $n = 8$	Max. Ag		Ave. $n = 3$			Ave. $n = 3$	
S	18.55	18.81	15.94	5.34	0.34	3.67	6.24	0.23
Se	0.23	0.21	1.54	0.87	0.12	0.33	0.63	0.00
Te	0.09	0.02	0.58	34.02	37.81	28.43	11.73	36.08
Ag	5.96	6.47	27.25	0.50	0.00	0.06	0.01	62.68
Pb	0.04	0.00	0.00	0.00	1.01	0.00	0.01	0.00
Sb	0.00	0.00	0.00	0.22	0.16	0.18	0.05	0.13
Cu	12.54	12.34	0.09	0.47	0.02	1.23	0.10	0.26
Ti	0.00	0.00	0.00	0.01	0.00	0.00	0.00	0.00
Cr	0.00	0.00	0.00	0.00	0.00	0.00	0.00	0.00
Fe	0.53	0.79	0.07	0.37	0.66	0.24	0.50	0.12
Zn	0.00	0.00	0.00	0.00	0.00	0.00	0.00	0.00
Cd	0.07	0.03	0.00	0.00	0.00	0.00	0.00	0.00
As	0.00	0.02	0.00	0.00	0.00	0.00	0.00	0.00
Mn	0.00	0.00	0.00	0.02	0.00	0.00	0.00	0.00
Bi	61.43	60.98	54.05	57.72	59.07	64.72	80.04	0.00
Ni	0.00	0.00	0.00	0.01	0.00	0.00	0.00	0.00
Co	0.00	0.00	0.00	0.01	0.79	0.01	0.00	0.00
W	0.00	0.00	0.00	0.04	0.00	0.00	0.01	0.00
Sn	0.00	0.00	0.00	0.00	0.00	0.00	0.00	0.00
In	0.00	0.00	0.00	0.00	0.00	0.00	0.00	0.00
Total	99.45	99.67	99.53	99.61	99.98	98.89	99.32	99.50
	S+Se+Te = 23		S+Se+Te = 2	S+Se+Te = 3	S+Se+Te = 1	S+Se+Te = 3	S+Se+Te = 3	S+Se+Te = 1
S	22.86	22.89	1.91	1.12	0.03	1.01	1.98	0.02
Se	0.12	0.10	0.07	0.07	0.00	0.04	0.08	0.00
Te	0.03	0.01	0.02	1.80	0.97	1.95	0.94	0.98
Ag	2.18	2.34	0.97	0.03	0.00	0.00	0.00	2.00
Pb	0.01	0.00	0.00	0.00	0.02	0.00	0.00	0.00
Sb	0.00	0.00	0.00	0.01	0.00	0.01	0.00	0.00
Cu	7.79	7.58	0.01	0.05	0.00	0.17	0.02	0.01
Ti	0.00	0.00	0.00	0.00	0.00	0.00	0.00	0.00
Cr	0.00	0.00	0.00	0.00	0.00	0.00	0.00	0.00
Fe	0.37	0.55	0.00	0.05	0.04	0.04	0.09	0.01
Zn	0.00	0.00	0.00	0.00	0.00	0.00	0.00	0.00
Cd	0.02	0.01	0.00	0.00	0.00	0.00	0.00	0.00
As	0.00	0.01	0.00	0.00	0.00	0.00	0.00	0.00
Mn	0.00	0.00	0.00	0.00	0.00	0.00	0.00	0.00
Bi	11.61	11.39	0.99	1.87	0.92	2.72	3.90	0.00
Ni	0.00	0.00	0.00	0.00	0.00	0.00	0.00	0.00
Co	0.00	0.00	0.00	0.00	0.04	0.00	0.00	0.00
W	0.00	0.00	0.00	0.00	0.00	0.00	0.00	0.00
Sn	0.00	0.00	0.00	0.00	0.00	0.00	0.00	0.00
In	0.00	0.00	0.00	0.00	0.00	0.00	0.00	0.00
Total	45.00	44.87	1.99	5.01	2.02	5.94	4.95	3.01

[1)] Cpx skarn, clinopyroxene skarn; Wo skarn, wollastonite skarn; Grt skarn, garnet skarn.

tween wollastonite skarn and limestone. The diopside occurs in the wollastonite skarn at the border between wollastonite skarn and limestone. Morphological feature and chemical characteristic of diopside are obviously different from the prismatic hedenbergite crystals of the main clinopyroxene skarn ore. It is possibly formed by the residual solution enriched in Mg and Fe at the end of skarnization or post mineralization stage.

Characteristic feature of ore and skarn minerals in the Eboshi deposit

The Naganobori copper skarn deposits have been categorized as a Cu-Zn(-Co)-W skarn deposit based on the

Table 3. Chemical compositions of selected skarn minerals

Skarn type[1]	Cpx skarn		Grt skarn		Wo skarn				Cpx skarn	Grt skarn		Wo skarn	
	Clinopyroxene								Garnet				
wt%	Ave.	Std.	Ave.	Std.	Cpx I Ave.	Cpx I Std.	Cpx II Ave.	Cpx II Std.		Ave.	Std.	Ave.	Std.
	n = 56		n = 19		n = 18		n = 25			n = 14		n = 15	
SiO_2	48.53	0.51	50.08	1.77	48.58	0.45	52.01	1.92	35.29	35.38	0.25	35.18	0.29
TiO_2	0.01	0.01	0.01	0.01	0.01	0.02	0.01	0.01	0.04	0.01	0.02	0.03	0.07
Al_2O_3	0.09	0.10	0.02	0.06	0.04	0.07	0.11	0.13	0.05	0.26	0.28	0.32	0.42
Cr_2O_3[2]	0.01	0.02	0.01	0.02	0.02	0.02	0.02	0.02	0.00	0.00	0.00	0.01	0.02
V_2O_3[2]	0.01	0.02	0.01	0.01	0.01	0.01	0.02	0.02	0.00	0.00	0.00	0.00	0.01
Fe_2O_3[2]	-		-		-		-		31.43	30.61	0.72	30.61	0.66
FeO[2]	25.83	1.69	19.34	5.84	25.84	1.64	12.00	6.64	-	-		-	
MnO[2]	1.67	0.59	1.37	0.77	1.72	0.66	1.62	2.22	0.05	0.11	0.05	0.23	0.17
MgO	0.69	0.92	4.94	4.22	0.75	0.70	9.51	5.14	0.02	0.08	0.05	0.02	0.03
CaO	22.60	0.36	23.40	0.82	22.62	0.34	24.09	0.90	32.94	33.03	0.24	33.01	0.21
Na_2O	0.10	0.06	0.06	0.00	0.04	0.05	0.04	0.05	0.00	0.01	0.01	0.00	0.01
K_2O	0.00	0.01	0.00	0.03	0.00	0.01	0.01	0.02	0.00	0.00	0.00	0.01	0.03
Total	99.56		99.23		99.63		99.44		99.82	99.49		99.44	
	O = 6								O = 12				
Si	2.00	0.01	2.00	0.01	2.00	0.01	2.00	0.01	2.99	3.00	0.02	2.99	0.02
Ti	0.00	0.00	0.00	0.00	0.00	0.00	0.00	0.00	0.00	0.00	0.00	0.00	0.00
Al	0.00	0.00	0.00	0.00	0.00	0.00	0.00	0.01	0.01	0.03	0.03	0.03	0.04
Cr^{3+}	0.00	0.00	0.00	0.00	0.00	0.00	0.00	0.00	0.00	0.00	0.00	0.00	0.00
V^{3+}	0.00	0.00	0.00	0.00	0.00	0.00	0.00	0.00	0.00	0.00	0.00	0.00	0.00
Fe^{3+}	-		-		-		-		2.00	1.95	0.04	1.96	0.05
Fe^{2+}	0.89	0.06	0.65	0.21	0.89	0.06	0.40	0.23	-	-		-	
Mn^{2+}	0.06	0.02	0.05	0.03	0.06	0.02	0.05	0.07	0.00	0.01	0.00	0.02	0.01
Mg	0.04	0.06	0.29	0.24	0.05	0.04	0.54	0.28	0.00	0.01	0.01	0.00	0.00
Ca	1.00	0.01	1.00	0.01	1.00	0.01	0.99	0.01	2.99	3.00	0.02	3.00	0.02
Na	0.01	0.00	0.00	0.00	0.00	0.00	0.00	0.00	0.00	0.00	0.00	0.00	0.00
K	0.00	0.00	0.00	0.00	0.00	0.00	0.00	0.00	0.00	0.00	0.00	0.00	0.00
Total	4.00		4.00		4.00		3.99		8.00	8.00		8.01	
		Range		Range		Range		Range			Range		Range
Hd[3]	89.9	76.0-98.2	66.3	22.9-97.7	89.4	73.2-94.8	40.4	7.5-86.4	Adr[3]	99.5	98.1	94.2-99.4	97.7	92.0-99.6
Di[3]	4.2	0.0-16.9	28.9	1.2-76.3	4.6	0.1-16.7		9.2-92.2	Grs[3]	0.3	1.3	0.0-5.6	1.6	0.0-7.3
Jo[3]	5.9	1.8-11.0	4.8	0.8-8.5	6.0	3.7-11.6	5.6	0.3-33.8	Sps[3]	0.1	0.3	0.0-0.5	0.6	0.2-1.8
									Prp[3]	0.1	0.3	0.0-0.8	0.1	0.0-0.4

[1] Cpx skarn, clinopyroxene skarn; Wo skarn, wollastonite skarn; Grt skarn, garnet skarn.
[2] Cr as Cr_2O_3, V as V_2O_3, Fe as Fe_2O_3 for garnet and as FeO for clinopyroxene, wollastonite, ilvaite and babingtonite, Mn as MnO.
[3] Hd, hedenbergite component; Di, diopside component; Jo, johannsenite component; Adr, andradite component; Grs, grossular component; Sps, spessartine component; Prp, pyrope component.

main ore minerals (Watanabe, 2009). Kato (1916) concluded that the large quantities of iron and silica have been introduced from the consolidating granite-porphyry magma to the limestone, and that the main deposit or the skarn mass has been formed by a process of metasomatism. The Co content of Hanano-yama porphyry after releasing Co as ore minerals have been reported as 3.8-7.4 ppm by Sasaki et al. (2014). In the study of the skarn deposits in the Tsumo mining area, Izawa (1981) has already suggested the decrease of metal elements in the granitic rocks due to the release of metal elements for the formation of deposits for the granite in the Tsumo mine. It is also noted that cobaltite has been only reported from the Eboshi and Imori skarn deposits (Fig. 1b), and that the Ni content in cobaltite from the Eboshi skarn deposit is from nil to very low (Table 2); but a preliminary data of cobaltite composition from the Imori skarn deposit is $(Co_{0.83}Ni_{0.14}Fe_{0.06})_{\Sigma 1.03}As_{0.99}(S_{0.99}Se_{0.01})$ (n =

Table 3. (Continued)

Skarn type[1]	Wo skarn		Cpx skarn		Grt skarn		Wo skarn		Cpx skarn	
	Wollastonite				Ilvaite				Babingtonite	
wt%	Ave.	Std.	Ave.	Std.	Ave.	Std.	Ave.	Std.	Ave.	Std.
	n = 13		n = 53		n = 5		n = 6		n = 3	
SiO_2	50.63	0.67	28.60	0.39	28.76	0.44	28.98	0.50	51.87	0.24
TiO_2	0.01	0.02	0.01	0.02	0.01	0.01	0.02	0.01	0.02	0.01
Al_2O_3	0.01	0.01	0.15	0.06	0.09	0.02	0.02	0.28	0.20	0.20
Cr_2O_3[2]	0.01	0.02	0.01	0.02	0.02	0.01	0.01	0.01	0.00	0.00
V_2O_3[2]	0.01	0.01	0.01	0.02	0.02	0.02	0.01	0.02	0.00	0.00
Fe_2O_3[2]	-		-		-		-		-	
FeO[2]	6.61	4.12	49.16	0.71	48.26	0.36	48.30	1.28	21.70	0.12
MnO[2]	1.19	0.55	2.14	1.57	2.70	0.54	2.58	0.71	2.52	0.19
MgO	0.04	0.03	0.03	0.02	0.05	0.06	0.21	0.02	0.27	0.10
CaO	40.80	3.82	13.42	0.14	13.51	0.29	13.41	0.59	19.41	0.04
Na_2O	0.01	0.01	0.01	0.01	0.01	0.01	0.01	0.01	0.02	0.03
K_2O	0.06	0.10	0.00	0.00	0.00	0.00	0.00	0.01	0.00	0.00
Total	99.39		93.54		93.43		93.55		96.01	
	O = 3				Σcations = 6				Σcations = 9	
Si	1.00	0.00	1.99	0.01	2.00	0.01	2.01	0.04	5.00	0.01
Ti	0.00	0.00	0.00	0.00	0.00	0.00	0.00	0.00	0.00	0.00
Al	0.00	0.00	0.01	0.01	0.01	0.00	0.00	0.02	0.02	0.02
Cr^{3+}	0.00	0.00	0.00	0.00	0.00	0.00	0.00	0.00	0.00	0.00
V^{3+}	0.00	0.00	0.00	0.00	0.00	0.00	0.00	0.00	0.00	0.00
Fe^{3+}	-		-		-		-		-	
Fe^{2+}	0.11	0.07	2.87	0.06	2.81	0.04	2.82	0.06	1.74	0.00
Mn^{2+}	0.02	0.01	0.13	0.09	0.16	0.03	0.15	0.04	0.20	0.02
Mg	0.00	0.00	0.00	0.00	0.01	0.01	0.02	0.00	0.04	0.01
Ca	0.86	0.07	1.00	0.01	1.01	0.01	1.00	0.04	2.00	0.00
Na	0.00	0.00	0.00	0.00	0.00	0.00	0.00	0.00	0.00	0.00
K	0.00	0.00	0.00	0.00	0.00	0.00	0.00	0.00	0.00	0.00
Total	1.99		6.00		6.00		6.00		9.00	
			Estimated Fe^{2+} : Fe^{3+} based on neutralization (apfu)							
		Fe^{3+}	1.01		0.99		0.98		0.98	
		Fe^{2+}	1.86		1.82		1.84		0.76	
		$Fe^{2+}/\Sigma Fe$	0.65		0.65		0.65		0.44	

[1] Cpx skarn, clinopyroxene skarn; Wo skarn, wollastonite skarn; Grt skarn, garnet skarn.
[2] Cr as Cr_2O_3, V as V_2O_3, Fe as Fe_2O_3 for garnet and as FeO for clinopyroxene, wollastonite, ilvaite and babingtonite, Mn as MnO.
[3] Hd, hedenbergite component; Di, diopside component; Jo, johannsenite component; Adr, andradite component; Grs, grossular component; Sps, spessartine component; Prp, pyrope component.

21) in average. The further investigation on the Co and Ni contents of cobaltite from the skarn deposits in the Akiyoshi mining area is mandatory.

It is noticed that scheelite and sphalerite in the ores from the Eboshi skarn deposit in the present study are rather small in quantity. Sporadically occurrence of scheelite has been reported by Kato (1916) and Ogura (1921). After Kato (1916), scheelite occurs only sparingly, but occasionally it is considerably concentrated in the skarn. It is commonly firmly imbedded in the clinopyroxene skarn but less common in the garnet and clinopyroxene-garnet skarns. It is consistent with the description of Ogura (1921), who found scheelite sporadically in clinopyroxene skarn from the Eboshi deposit. The well-crystallized scheelite crystals with a pyramidal habit range from the microscopic size to several centimeters in length

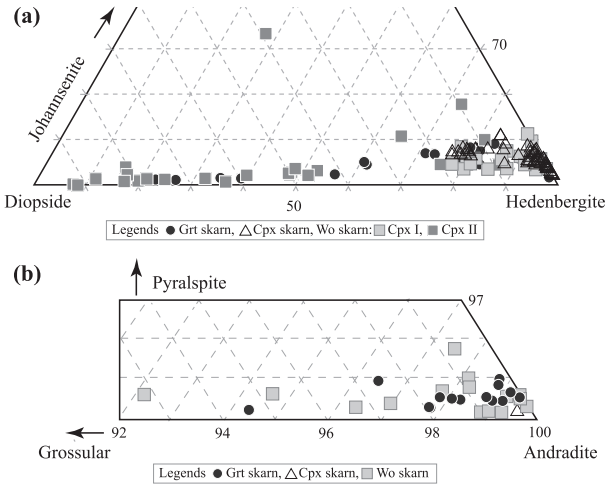

Figure 6. Johannsenite–diopside–hedenbergite and pyralspite–grossular–andradite diagrams for (a) clinopyroxene and (b) garnet, respectively.

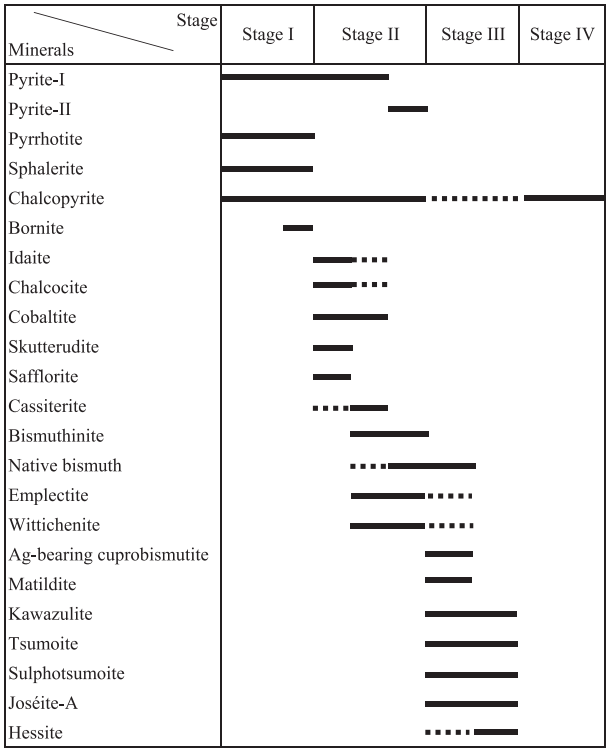

Figure 7. Mineralization sequence for the Eboshi deposit in this study.

(Kato, 1916). Kato (1916) concluded that scheelite belongs to the earliest crystallization of all minerals found in the Eboshi deposit. However, no Zn-rich minerals have been described by Kato (1916) and Ogura (1921). Considering that zinc ore is produced from the Akaono deposit locating at ~ 2 km north of the Naganobori mining district (Fig. 1), and that the abundant oxidized Zn ores (>10 tons) were excavated from Zeniya archeological sites locating 1 km NNE from the Akaono deposit (Izawa et al., 2005), it is considered that zinc concentrates sporadically or regionally in the skarn deposits distributed in the Akiyoshi limestone region.

Table 4. Average chemical composition of fluorapophyllite-(K)[1)]

wt%	Ave.	Std.		Ave.	Std.
SiO_2	53.27	0.40	Si	8.00	0.01
Al_2O_3	0.02	0.04	Al	0.00	0.01
FeO[2)]	0.02	0.02	Fe^{2+}	0.00	0.00
MnO[2)]	0.05	0.05	Mn^{2+}	0.01	0.01
MgO	0.02	0.03	Mg	0.01	0.01
CaO	24.75	0.25	Ca	3.98	0.02
Na_2O	0.06	0.03	Na	0.02	0.01
K_2O	5.07	0.10	K	0.97	0.02
F	2.27	0.15	Total	12.98	
Total	85.53		F	1.08	0.07
Ex.O	0.96				
Total - Ex.O	84.57				

[1)] Cations are normalized as Si + Al = 8. Number of analytical points = 9.
[2)] Fe as FeO, Mn as MnO.

The minor Bi-, Ag-, and Te-bearing ore minerals identified newly in the present study are also important to characterize the Eboshi deposit. For example, in case of the Yamato skarn deposit, the characterization as a W-Mo-Cu-type Bi-bearing skarn deposit associated with ilmenite-series granitic rocks by Ishihara (2008) and as Cu-Ag-bearing deposit by Shimazaki (1980) was proved by Nagashima et al. (2016) who identified Ag- and/or Bi-bearing minerals such as bismuthinite, matildite, the Ag-Pb-Bi sulfate, and argentite. In addition, the Te-bearing mineral, joséite-A was reported from the skarn deposit of the Yamato mine by Ohnishi et al. (2007). Since we identified Ag-, Bi, and/or Te-bearing minerals, such as emplectite, wittichenite, Ag-bearing cuprobismutite, matildite, kawazulite, tsumoite, sulphotsumoite, joséite-A, and hessite, from the ores of the Eboshi deposit, the Eboshi skarn deposit is categorized as Cu-Co-Zn-W-type Bi-Ag-Te-bearing skarn deposit as well as the Yamato skarn deposit. Moreover, minor Bi-, Ag-, and Te-bearing minerals, such as native bismuth, bismuthinite, hedleyite, and hessite, also occur in the Tsumo mine (Sugaki et al., 1981) which was categorized as Cu-Zn-W skarn deposit by Watanabe (2009).

On the other hand, the Kiwada, Fujigatani, and Kuga mines locating in the Kuga district, eastern part of Yamaguchi Prefecture are categorized as the skarn type Cu-Sn-W deposits (Watanabe, 2009). Main ore minerals

of the Kiwada skarn deposit are pyrrhotite, chalcopyrite, scheelite, sphalerite, cassiterite, and pyrite (Nagahara, 1978). The Bi-, Ag-, and Te-bearing minerals have not been reported. The ore minerals from the Fujigatani skarn deposit are scheelite, pyrrhotite, and chalcopyrite along with pyrite, arsenopyrite, sphalerite, galena, molybdenite, native bismuth, bismuthinite, and cassiterite (Hakari, 1960; Ito, 1962; Shimazaki, 1977; Sato, 1980). The ores from the Kuga skarn deposit consist mainly of pyrrhotite, chalcopyrite, and sphalerite, along with minor pyrite, marcasite, arsenopyrite, galena, scheelite, native bismuth, bismuthinite, stannite, and cassiterite (Higashimoto, 1977; Sawai and Kimura, 1992; Kase et al., 1993). No Ag- and Te-bearing minerals have been reported from these Cu-Sn-W skarn deposits in spite of the similar main ore mineral assemblages to those of the Eboshi skarn deposit.

Clinopyroxene, garnet, wollastonite, and ilvaite are common skarn minerals in both the Eboshi and Yamato deposits. Some skarn minerals, such as babingtonite in the Eboshi skarn deposit and epidote, vesuvianite, and malayaite in the Yamato skarn deposit, are not common in both deposits, probably due to the limited samples studied.

Implications for ore mineralization in the San-yo Belt

Not a few skarn deposits are developed in and around the Akiyoshi Plateau by the intrusions of Cretaceous ilmenite-series granitic magma into the limestone (e.g., Kato, 1916; Suzuki, 1932). These skarn deposits are assumed to show similar characteristics in terms of the mineral assemblages and their occurrences due to the relation between host rock and felsic magmatic activity in common. However, the regional differences have been pointed out as mentioned before (e.g., Sekine, 1958; Miyake and Akatsuka, 1963). Therefore, the characteristics of the skarn deposits in the Akiyoshi limestone area are comprehensively evaluated based on the general and individual characteristics of the mineral assemblages and occurrences in the ore deposits of the Naganobori copper mine generated by the Hanano-yama granite porphyritic activity and Yamato skarn deposit generated by the Ofuku granitic activity (Sasaki et al., 2014, 2016), as well as the characteristics of other previously reported deposits in this area.

General characteristics of the skarn deposits in the Akiyoshi limestone district are as follows;

(1) Major ore minerals are commonly pyrite, chalcopyrite, bornite, cobaltite, sphalerite, and scheelite. However, the abundances of sphalerite, scheelite, and cobaltite are variable for each deposit. Although sphalerite and scheelite scarcely occur in our specimens from the Eboshi skarn deposit, they are the major ore minerals in this deposit in Kato (1916) and Ogura (1921). Three types of skarns, that is clinopyroxene skarn, garnet skarn, and wollastonite skarn, are also common.

(2) Accessary ore minerals containing Ag, Bi, Te, ±Au occur in the skarn deposits of both the Eboshi and the Yamato mines. These ore minerals occur in the interstices and cavities of major ore minerals, indicating that they were formed after major ore minerals. The low temperature hydrothermal solution produced various Ag, Bi, Te, ±Au mineral species, but their quantity is small.

(3) The occurrence and mineralization sequence of the major and minor minerals of the skarn deposits in the Akiyoshi district, summarized in (1) and (2), respectively, are similar to those in the San-in district, e.g., the skarn deposits of the Tsumo mine (Sugaki et al., 1981). Thus, the skarn deposits associated with ilmenite-series granitoids in the San-yo and San-in districts show common geological, mineralogical, and ore geological features.

ACKNOWLEDGMENTS

We thank the Editor Dr. M. Fukuyama, as well as two anonymous reviewers for their constructive comments, Mr. Y. Ikeda, director of Naganobori Copper-mine and Culture Center, for his permission for sample collection, Prof. M. Akasaka for his constructive comments, and Mr. Y. Morifuku of the Centre for Instrumental Analysis, Yamaguchi University for his technical support. This study was partly supported by a research grant for Yamaguchi-gaku project of Yamaguchi University. This study was also supported by JSPS KAKENHI Grant Number JP18K03782 to M.N.

SUPPLEMENTARY MATERIAL

Color version of Figure 5 is available online from https://doi.org/10.2465/jmps.200818.

REFERENCES

Hakari, N. (1960) Geology and ore deposits of the Fujigatani mine, Yamaguchi Prefecture-Several problems on the form of the ore body and structural control. Mining Geology, 10, 94-104 (in Japanese with English abstract).

Higashimoto, S. (1977) Geology and ore deposits of the Kuga mine, Southwest Japan. Bulletin of the Geological Survey of Japan, 28, 775-793 (in Japanese with English abstract).

Hirabayashi, T. (1909) On the ore-deposits containing Ni and Co

ores. Journal of the Mining Institute of Japan, 25, 1049–1073 (in Japanese).

Ikeda, Y. (2015) Remains of the Naganobori copper mine: The oldest ancient copper mine in Nagato, Japan. Nihon no Iseki, 49. pp. 194, Doseisha, Tokyo, (in Japanese).

Ishihara, S. (2008) On bismuth resources of Japan and world. Shigen–Chishitsu, 58, 131–138 (in Japanese with English abstract).

Ito, K. (1962) Zoned skarn of the Fujigatani mine, Yamaguchi Prefecture, Japan. Journal of Geology and Geography, 33, 169–190.

Izawa, E. (1981) Chemical characteristics of the granitic rocks in the Tsumo mining district, southwestern Japan. Mining Geology Special Issue, 9, 23–30 (in Japanese with English abstract).

Izawa, E., Yoshikawa, R. and Nakanishi, T. (2005) Forgotten Zn ores: Zn sulfate minerals–Investigation report of the remains of the Akaono Ag–Cu mine, Yamaguchi Prefecture. Abstracts I of the Mining and Materials Processing Institute of Japan (MMIJ) Annual Meeting 2005, Resource 17, Kikaku. 125–128, G–1 (in Japanese).

Kase, K., Natori, J. and Shimazaki, H. (1993) Mineralogical study of skarn type Cu–W deposit at the Kuga mine, Yamaguchi Prefecture, Japan. Resource Geology, 43, 255–266.

Kato, T. (1916) The Ore Deposits in the Environs of Hananoyama, near the Town of Oda, Province of Nagato, Japan. The Journal of the Meiji College of Technology, 1, 1–95.

Kato, T. (1937) New geology of ore deposits. pp. 757, Fuzambo, Tokyo (in Japanese).

Miyake, H. and Akatsuka, K. (1963) Geological notes of the Yamato mine, Yamaguchi Prefecture. Geological Report of the Hiroshima University, 12, 381–399.

Nagahara, M. (1978) Geology, ore deposits and some guides to prospecting of the Kiwada tungsten mine, Yamaguchi Prefecture. Mining Geology, 28, 373–384 (in Japanese with English abstract).

Nagashima, M., Akasaka, M. and Morifuku, Y. (2016) Ore and skarn mineralogy of the Yamato mine, Yamaguchi Prefecture, Japan, with emphasis on silver–, bismuth–, cobalt–, and tin–bearing sulfides. Resource Geology, 66, 37–54.

Nakamura, K. (1954) Cobalt ores. In Mineral Resources of Japan, BI–c, Geological Survey of Japan, 103–114.

Nambu, M., Tanida, K., Kitamura, T. and Sakurai, K. (1970) Heterogenite from Naganobori Mine, Yamaguchi Prefecture, Japan. The Journal of the Japanese Association of Mineralogists, Petrologists and Economic Geologists, 64, 53–63 (in Japanese with English abstract).

Ogura, T. (1921) Investigation report of the Naganobori mine and Oda mine. Report, Geological Survey of Japan, 82, 49–72 (in Japanese).

Ohnishi, M., Kusachi, I., Kobayashi, S., Fujiwara, Y. and Nishida, K. (2007) Preisingerite from the Yamato mine, Yamaguchi Prefecture, Japan. Japanese Magazine of Mineralogical and Petrological Sciences, 36, 61–65 (in Japanese with English abstract).

Ota, M. (1976) Geological map of the Akiyoshi district. Bulletin of the Akiyoshi–dai Museum of Natural History, 12, 1–34.

Sasaki, Y., Imaoka, T., Nakashima, K. and Fujikawa, M. (2014) Geochemical characteristics and fluid inclusions of intrusive rocks in the Akiyoshi Limestone, and their bearing on mineralization. Bulletin of the Akiyoshi–dai Museum of Natural History, 49, 7–23 (in Japanese with English abstract).

Sasaki, Y., Imaoka, T., Nagashima, M., Nakashima, K., et al. (2016) The Cretaceous Ofuku pluton and its relation to mineralization in the Western Akiyoshi Plateau, Yamaguchi Prefecture, Japan. Resource Geology, 66, 85–113.

Sato, K. (1980) Tungsten skarn deposit of the Fujigatani Mine, Southwest Japan. Economic Geology, 75, 1066–1082.

Sawai, O. and Kimura, H. (1992) Skarn from the Iwaya ore body, Kuga mine, Yamaguchi Prefecture, Japan. Commemorative Papers for Professor Yukio Matsumoto, 285–292 (in Japanese with English abstract).

Sekine, Y. (1958) Wollastonite ores in the pyrometasomatic copper–tungsten deposits at the Yamato mine, Yamaguchi Prefecture. Bulletin of the Geological Survey of Japan, 9, 675–688 (in Japanese with English abstract).

Shimazaki, H. (1968) Genesis of pyrometasomatic ore deposits of the Tsumo mine, Shimane Prefecture. Japanese Journal of Geology and Geography, 39, 73–78.

Shimazaki, H. (1977) Grossular–spessartine–almandine garnets from some Japanese scheelite skarns. Canadian Mineralogist, 15, 74–80.

Shimazaki, H. (1980) Characteristics of skarn deposits and related acid magmatism in Japan. Economic Geology, 75, 173–183.

Sugaki, A., Soeda, A., Shima, H., Kitakaze, A., et al. (1981) Ore deposits and minerals of the pyrometasomatic deposit of the Tsumo mine, with special reference to Maruyama deposit. Mining Geology Special Issue, No. 9, 89–144 (in Japanese with English abstract).

Suzuki, J. (1932) The contact metamorphic ore deposits in the environs of the Ofuku mine, province of Nagato, Japan. Journal of Faculty of Science, Hokkaido Imperial University, Series 4, Geology and Mineralogy, 70, 750–769.

Ueda, K. (2002) Copper production at Naganobori mine for Nara Buddha construction in the first half of 8th century and its development afterwards. Fifth International Conference on the Beginnings of the Use of Metals and Alloys, Gyeongju, Korea, 21–24, 19–27.

Watanabe, M. (2009) Naganobori mine. In Chugoku (Editorial Committee of Chugoku, Geological Society of Japan Eds.). Regional Geology of Japan, 6. Asakura Publishing Company, 453–454 (in Japanese).

Manuscript received August 18, 2020
Manuscript accepted December 27, 2020
Published online February 10, 2021
Manuscript handled by Mayuko Fukuyama